Quaternary Science Reviews 331 (2024) 108650

Contents lists available at ScienceDirect

Quaternary Science Reviews

journal homepage: www.elsevier.com/locate/quascirev

# Vegetation and glacier dynamics are sensitive to summer (not winter) warming and the evidence for larch refugia in the 'Northern Pole of Cold' inferred from sedimentary ancient DNA and geochemistry

Weihan Jia [a,b], Boris K. Biskaborn [a], Kathleen R. Stoof-Leichsenring [a], Luidmila A. Pestryakova [c], Ulrike Herzschuh [a,b,d,*]

[a] Polar Terrestrial Environmental Systems Research Group, Alfred Wegener Institute Helmholtz Centre for Polar and Marine Research, Potsdam, Germany
[b] Institute of Environmental Science and Geography, University of Potsdam, Potsdam, Germany
[c] Department for Geography and Biology, North-Eastern Federal University of Yakutsk, Yakutsk, Russia
[d] Institute of Biochemistry and Biology, University of Potsdam, Potsdam, Germany

ARTICLE INFO

Handling Editor: Dr. Yan Zhao

*Keywords:*
Sedimentary ancient DNA (sedaDNA)
Oymyakon
Metabarcoding
Glacial activity
Vegetation dynamics
Glacial refugia
*Larix*
Summer warming
Paleoecology

ABSTRACT

Climate seasonality critically influences the functioning and dynamics of ecosystems in continental areas. The ecological importance of winter temperatures on high-latitude vegetation changes has recently been argued to be largely overlooked in comparison to summer temperatures. The Oymyakon region from eastern Siberia, with its strong continentality of extremely cold winters and moderately warm summers, is ideally suited to study the response of past vegetation to seasonal temperature changes based on long ecological time-series. However, few paleorecords are available from this area. The history of regional glacial activity and potential plant refugia since Marine Isotope Stage (MIS) 3 is not well understood. Here, we present geochemical and plant DNA metabarcoding records retrieved from a sediment core from Lake Ulu in the Oymyakon region, which provides detailed information on glacier and vegetation dynamics over the last 43 cal. ka BP. Our results suggest that glacial fluctuations were primarily driven by summer insolation, and Lake Ulu was likely initiated by glacial retreat during MIS 3. The catchment experienced multiple glacial advance/retreat cycles until the Last Glacial Maximum, and the glaciers fully retreated by 20 cal. ka BP. In addition, a tundra-steppe landscape dominated by *Dryas*, *Papaver*, Saliceae, and Anthemideae occupied the catchment for most of the time and began to collapse around 19 cal. ka BP following the expansion of trees and shrubs such as *Larix*, *Betula*, *Alnus*, and *Vaccinium*. Postglacial plant assemblages in the Oymyakon region exhibit a high sensitivity to summer temperature variations, with minimal impact from winter temperatures. This can be explained by the dominance of summer insolation amplitude, extreme continentality, extended plant growing season, and plant genetic adaptation to cold. Notably, our ancient DNA record show the earliest postglacial expansion of larch in eastern Siberia (around 18.6 cal. ka BP), which is likely related to the presence of local refugia. This implies that the Oymyakon region may be one of the earliest sources for larch recolonization and that more research should be implemented to provide insights into larch expansion and migration, and to better predict the future scenarios for Siberian larch forests.

## 1. Introduction

Temperature is increasing at unprecedented rates across most of the high-latitude regions (IPCC, 2023) mainly due to polar amplification (Miller et al., 2010). Climate seasonality, especially changes in summer and winter temperature, plays a critical role in influencing the functioning and dynamics of terrestrial ecosystems (Kwiecien et al., 2022; White and Hastings, 2020). Contrasting patterns of summer and winter temperature changes at high latitudes have been found at orbital and suborbital scales, either in proxy data or climate models, which can be explained mainly by differences in seasonal trends of solar insolation (Kaufman and Broadman, 2023; Meyer et al., 2015). Currently, winter is

* Corresponding author. Polar Terrestrial Environmental Systems Research Group, Alfred Wegener Institute Helmholtz Centre for Polar and Marine Research, Telegrafenberg A45, Potsdam 14473, Germany.
*E-mail address:* Ulrike.Herzschuh@awi.de (U. Herzschuh).

https://doi.org/10.1016/j.quascirev.2024.108650
Received 28 November 2023; Received in revised form 26 March 2024; Accepted 27 March 2024
Available online 11 April 2024

warming much faster than summer at latitudes above 50°N (Xia et al., 2014), consistent with increasing winter insolation in the late Holocene (Kaufman and Broadman, 2023). However, the ecological consequences of seasonally non-uniform changes in temperature are not yet fully understood.

In recent years, a growing number of reviews and studies have emphasized that the importance of winter temperatures in altering spatial and temporal patterns of high-latitude vegetation has been largely underestimated (Cooper, 2014; Kreyling et al., 2019; Niittynen et al., 2020; Rapacz et al., 2014; Sanders-DeMott and Templer, 2017; Williams et al., 2015). Low winter temperatures can lead to physical and biological damage to plant cells (Griffith and Yaish, 2004) and changes in plant-community composition due to species-specific differences in physiological and genetic adaptations to seasonal temperature variations (Williams et al., 2015). Warm winters can result in shallower snow cover and higher soil temperatures, which can promote plant biomass and growth, but expose plants to additional frost damage and pathogen invasion (Cooper, 2014; Rapacz et al., 2014). On the other hand, summer temperature has long been recognized as a key factor in regulating changes in vegetation productivity and composition at high latitudes as summer is the peak season for plant photosynthesis and growth (Berner et al., 2020; Elmendorf et al., 2012; Zhang et al., 2022). In light of these contrasting arguments, understanding vegetation dynamics in relation to seasonal temperature variations based on long ecological time-series serves as a valuable reference for our assessment of terrestrial ecosystem development in a changing climate.

*Larix* is a light- and warmth-demanding boreal tree taxon and its growth is sensitive to seasonal temperature changes. Different *Larix* species in the high latitudes of the Northern Hemisphere share a similar range of dominance at July temperatures of around 9–10 °C, but differ in their tolerance of low January temperatures, varying from −8 °C to −45 °C (Schulte et al., 2022a). Today, *Larix* is the most widespread and dominant taxon in eastern Eurasia (Herzschuh, 2020), but we still lack understanding of the past survival and distributional range of larch and its postglacial expansion and migration trajectories in eastern Siberia. For example, the low and intermittent occurrence of larch during the Last Glacial Maximum (LGM) in eastern Siberia has been captured by pollen, macrofossil, and a few ancient DNA records (reviewed by Schulte et al., 2022a), but such results may have been underestimated because of underrepresentation and poor preservation of *Larix* pollen (Niemeyer et al., 2015; Sjögren et al., 2008) and low abundance of macrofossils. Furthermore, previous studies argue that northern refugia have played an important role in supporting the dominance of *Larix* in Siberia since the LGM (Binney et al., 2009; Brubaker et al., 2005; Herzschuh, 2020; Lozhkin et al., 2018; Schulte et al., 2022a), but few glacial refugia have been reported from eastern Siberia.

The Oymyakon Upland, located in the mountainous region of southern Yakutia, is known as the 'Northern Pole of Cold' and is one of

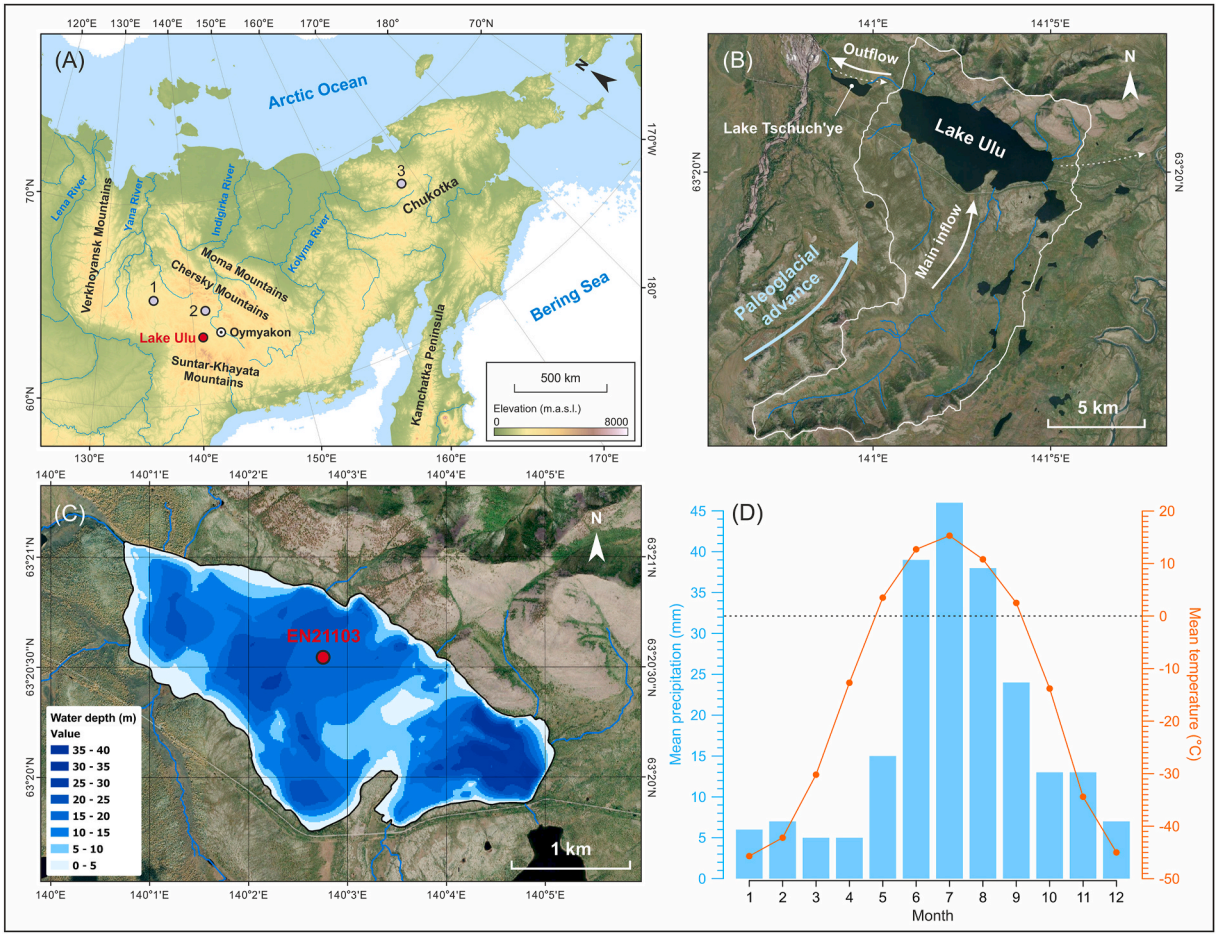


**Fig. 1.** (A) Map showing the locations of Lake Ulu, Oymyakon, and other sites (purple points) mentioned in this paper, including (1) Lake Emanda (Schulte et al., 2022b), (2) Lake Smorodinovoye (Anderson et al., 2002), and (3) Lake Ilirney (Vyse et al., 2020). Light blue shading shows the approximate location of the coastline during the Last Glacial Maximum (LGM) when sea level was 120 m lower than the present (generated based on Assis et al., 2018). (B) Map of the catchment area of Lake Ulu (white line). The white arrows point to the flow direction of current rivers. The dashed arrows point to the possible past flow direction of the Kyubyume River, which now flows northward to bypass the Lake Ulu catchment because of glacial dams formed during MIS 4 (Lozhkin et al., 2018). (C) The coring site of Lake Ulu (EN21103). Bathymetry was measured in 2021. (D) Morden climate data from Oymyakon meteorological station, showing the mean monthly temperature and precipitation (sourced from http://www.pogodaiklimat.ru). The dashed line denotes 0 °C.

the coldest areas of the Northern Hemisphere. One of the lowest air temperatures ever measured in the Northern Hemisphere (−67.8 °C) was officially recorded in Oymaykon in 1933 (http://wmo.asu.edu/content/asia-lowest-temperature). This region has an extremely continental climate and the highest temperature amplitude (Isaia, 2016), with an annual temperature range of more than 60 °C. The geomorphology was extensively modified by Late Quaternary glaciation, especially during the LGM (Barr and Clark, 2012). Modern vegetation is classified within the north taiga zone and *Larix* forests. This area is therefore ideally suited to study the dynamics of mountain glaciers and vegetation and their relationships to seasonal temperature changes, and to identify potential larch refugia. Few studies have been performed in the Oymyakon region to date and continuous paleoecological records at a high taxonomic resolution are still scarce. For example, Lozhkin et al. (2018) speculate that *Larix* forests may have established earlier than 13.8 calibrated thousand years before the present (cal. ka BP) and expanded from local refugia based on the pollen data from Lake Tschuch'ye (Fig. 1B), but this record is restricted by the inherent limitation of *Larix* pollen and relatively short time-series.

Over the last two decades, sedimentary ancient DNA (sedaDNA) technologies has been successfully applied to uncover past changes in plant communities at multiple timescales (Dalén et al., 2023). Compared to fossil pollen, plant DNA from lake sediments is identifiable to a higher taxonomic resolution and provides local and catchment information on species composition (Alsos et al., 2018; Giguet-Covex et al., 2019; Jia et al., 2022). The P6 loop region of the chloroplast *trn*L (UAA) intron (Taberlet et al., 2007) is an optimal marker to maximize taxonomic resolution and diversity for vascular plants with appropriate reference databases and has been widely used by the community (Capo et al., 2021; Garcés-Pastor et al., 2023; Liu et al., 2021; Revéret et al., 2023; Stoof-Leichsenring et al., 2020). In addition, previous studies show that this marker captures the *Larix* DNA signal well from lake sediments (Niemeyer et al., 2017; Sjögren et al., 2017).

In this study, we present results of geochemical and plant DNA metabarcoding analyses of an 11-m-long sediment core covering approximately the last 43 cal. ka BP from Lake Ulu in the Oymyakon region. This paper aims (i) to reconstruct the history of glacial fluctuations in the lake catchment; (ii) to understand whether long-term vegetation compositional changes were driven by variations in summer or winter temperatures; and (iii) to explore the timing of postglacial expansion in larch and its relationship to potential glacial refugia.

## 2. Materials and methods

### 2.1. Study region

Lake Ulu (approximately 63°20'−63°21′N and 141°1'−141°5′E, 950 m above sea level [a.s.l.]), a freshwater lake with a present-day pH of 7.6 and an electrical conductivity of 73.4 μS $cm^{-1}$, is situated on the Oymyakon Upland (Fig. 1A) and the continuous permafrost zone of Siberia (Brown et al., 2002). The area of the lake is approximately 4.8 $km^2$, with a catchment of approximately 35.4 $km^2$. According to a seismic profile of the lake bottom in 2021, the lake is deepest in the southeast, where the maximum depth is approximately 35–40 m (Fig. 1C). The lake is fed mainly by a river that originates in the southern mountains (above 1370 m a.s.l.) and drains into the Kyubyume River via Lake Tschuch'ye at its northwestern shore (Fig. 1B), which in turn flows east into the Indigirka River. The ice limit of Marine Isotope Stage (MIS) 4 is identified in the northern mountains of the lake catchment (Ministry for Natural Resources and Ecology of the Russian Federation, 2014). Glacial (morainic) deposits are present across the catchment, which suggests that the area was broadly influenced by historical glacial activity (Ministry for Natural Resources and Ecology of the Russian Federation, 2011, 2014; Lozhkin et al., 2018).

Modern vegetation in the lake catchment is dominated by open larch forests (*Larix cajanderi* and *Larix gmelinii*; the name *Larix cajanderi* is not yet universally recognized and the classification of the two species is not very clear), which are dense on the mountain slopes and in the valley bottoms (Miesner et al., 2022). Understory shrubs are dominated by species of Ericaceae, *Vaccinium vitis-idaea*, and *Salix*. The ground is covered by mosses and lichen species along with dwarf shrubs such as Ericaceae and *Vaccinium vitis-idaea*. Modern meteorological records in Oymyakon (around 88 km from the lake, 800 m a.s.l.) give a mean annual temperature of −14.9 °C, a mean January temperature of −45.7 °C, a mean July temperature of 15.3 °C, and a mean annual precipitation of 218 mm (Fig. 1D; http://www.pogodaiklimat.ru), indicating an extremely cold and dry climate.

### 2.2. Field work and core subsampling

During August 2021, an 11-m-long sediment core (EN21103) was collected from the center of Lake Ulu at a water depth of 17.4 m (Fig. 1C) using the UWITEC 90 mm Hybrid piston coring system. Before coring, a coring site with around 11 m of continuous and undisturbed sediments was identified by performing parametrical sub-bottom profiling using an Innomar SES-2000 compact (Supplementary file S1; Wunderlich and Müller, 2003). During coring, coarse-grained sands were found at the bottom of the sediment core at a penetration depth of 11 m, indicating that the coring had likely reached the age of lake formation. A short core (EN21101-3, 15 cm) was also collected parallel to the long core using a UWITEC gravity corer. The short core was subsampled at 0.5-cm intervals in the field, and the topmost surface sample (0−0.5 cm) was radiocarbon ($^{14}C$) dated to detect potential reservoir effects. All sediment segments were transferred and stored at 4 °C at Alfred Wegener Institute Helmholtz Centre for Polar and Marine Research (AWI) in Potsdam.

Sediment segments were subsequently opened and subsampled in a cleaned and cooled laboratory (4 °C). The subsampling protocol was under strict hygienic rules to prevent contamination with modern DNA (see Epp et al., 2019 or Stoof-Leichsenring et al., 2022 for details). In total, 72 samples were collected for geochemical analyses. Seventy-one samples for sedaDNA analysis were taken from the interior of the sediment core and frozen at −20 °C until DNA extraction, and each covered a 2-cm thickness of sediment.

### 2.3. Geochemical analyses

Freeze-dried and milled samples were analyzed for total carbon (TC), total organic carbon (TOC), total inorganic carbon (TIC), and total nitrogen (TN) at the Carbon and Nitrogen Laboratory of AWI in Potsdam. TC, TOC, and TIC were measured using a soli TOC cube (Elementar). TN was measured using a rapid MAX N exceed (Elementar). The minimum detectable concentration for natural sediment samples is 0.1% for both machines. Carbonate-free samples were processed for the determination of stable carbon isotope composition of organic matter ($\delta^{13}C_{org}$). The $\delta^{13}C_{org}$ was measured using a Delta V Advantage Mass Spectrometer at the ISOLAB Facility of AWI in Potsdam. All isotopic values are reported in standard δ-notation in per mil (‰) relative to VPDB.

Non-destructive X-ray fluorescence (XRF) scanning measurements on split long core surfaces were performed with an AvaaTech XRF core scanner at AWI in Potsdam. All elements were measured at X-ray voltages of 10 kV and 30 kV and currents of 0.45 mA and 0.15 mA, respectively, with a step size of 0.5 cm and an exposure time of 10 s. The data are semiquantitative and provide relative fluctuations in the chemical element compositions as counts per second (cps). Raw element intensities were centered log-ratio (CLR) transformed and element ratios were additive log-ratio (ALR) transformed to reduce closed-sum effects (Croudace and Rothwell, 2015; Weltje and Tjallingii, 2008) using the *clr* and *alr* functions in the R-package *compositions* (van den Boogaart et al., 2023).

### 2.4. Radiocarbon dating

Due to the lack of observed terrestrial plant macrofossils in the core, the $^{14}$C dating was performed on the TOC content of 40 bulk sediment samples using accelerator mass spectrometry (AMS) at the MICADAS (Mini Carbon Dating System) Laboratory of AWI in Bremerhaven (Table 1; Mollenhauer et al., 2021). The age-depth model was based on the Bayesian method (Blaauw and Christen, 2011) and calibrated using the IntCal20 dataset (Reimer et al., 2020) via the *Bacon* function in the R-package *rbacon* (Blaauw et al., 2023). A reservoir effect of approximately 351 ± 24 $^{14}$C years has been determined by the dated surface sample (0−0.5 cm) from the short core. We assumed a constant $^{14}$C reservoir effect over time and therefore subtracted a value of 351 years from all $^{14}$C ages before calibration.

### 2.5. SedaDNA analyses

DNA extraction was carried out in the paleogenetic laboratories at AWI in Potsdam. Approximately 5 g of wet sediment was taken from the samples and processed using the DNeasy PowerMax Soil Kit (Qiagen), following the protocol of Zimmermann et al. (2017). One DNA extraction batch included 9 sediment samples and one extraction control (without sediment samples), and both were processed in the same way. DNA extracts from the samples were purified and concentrated using the GeneJET PCR Purification Kit (Thermo Scientific). PCR was performed with the "*g*" and "*h*" universal plant primers for the P6 loop region of the chloroplast *trn*L (UAA) intron (Taberlet et al., 2007). PCR setup followed the protocol of Baisheva et al. (2023). We produced three PCR replicates for sediment samples and DNA extraction controls and added a PCR negative template control (NTC) in each PCR replicate batch. After evaluation of PCR results via gel electrophoresis (2% agarose), PCR products were purified using the MinElute PCR Purification Kit (Qiagen) and pooled in equimolar concentrations. DNA concentrations of DNA extracts and purified PCR products were measured with the Qubit 4.0 fluorometer (Invitrogen), and the results showed no obvious contamination during the laboratory work. Library preparation and next-generation sequencing (2 × 150 bp) on the Illumina NextSeq 500 platform were performed with two independent sequencing runs at Fasteris SA, Switzerland (Sequencing batches APMG-59 and APMG-62; https://www.ebi.ac.uk/ena/browser/view/PRJEB70434). The data from the two runs were merged into a single dataset for the final interpretation.

Raw sequence data were processed by the OBITools3 package (Boyer et al., 2016; http://git.metabarcoding.org/obitools/obitools3; the tag files and script are available in Supplementary files S4 and S5), which includes *illuminapairedend* to align forward and reverse reads and then *ngsfilter* to assign the sequences to the PCR products based on their different tag combinations. We used *obiuniq* to merge duplicated sequences. The *obiclean* program was run with an *r* value of 0.05 to remove putative PCR or sequencing errors. Taxonomic assignments with *ecotag* were performed based on the 'SibAla_2023' customized reference database without a defined identity threshold. Basically, the 'SibAla_2023' database has been compiled from the following steps (Courtin et al., 2024; in revision). (i) Taxa selection from a given region (55–90°N, 50–150°E and 40–90°N, 150°E−140°W) and taxa occurrences (>10) using the Global Biodiversity Information Facility (GBIF) resulting in 233 families, 1059 genera, and 4849 species. Crop plant taxa (e.g., potatoes and tomatoes) are excluded. (ii) Alignment between selected taxa and available P6 loop sequences from public databases (the Arctic-Boreal vascular plant and bryophyte database, Sønstebø et al., 2010; Soininen et al., 2015; Willerslev et al., 2014; the European Molecular Biology Laboratory (EMBL) nucleotide database version 143, Kanz et al., 2005; the PhyloNorway database, Alsos et al., 2022). (iii) Quality filtering of selected P6 loop sequences. (iv) Preparation for use with *ecotag*. The 'SibAla_2023' database has a taxonomic coverage of 95.7% (family level), 89.4% (genus level), and 70.1% (species level),

**Table 1**
AMS$^{14}$C ages obtained from Lake Ulu sediment cores. Samples marked with asterisk are not included in the age model calculation.

| Lab ID | Composite depth (cm) | Dated material | $^{14}$C age (yr BP) | Reservoir effect corrected and calibrated age (95% confidence interval; cal. yr BP) |
|---|---|---|---|---|
| 10442.1.1 | 0–0.5 | TOC | 351 ± 24 | – |
| 9255.1.1 | 15 | TOC | 2995 ± 52 | 2546–2870 |
| 10443.1.1 | 25 | TOC | 4052 ± 26 | 3933–4145 |
| 9256.1.1 | 35 | TOC | 6932 ± 53 | 7425–7570 |
| 10444.1.1 | 45 | TOC | 7975 ± 29 | 8375–8510 |
| 9257.1.1 | 55 | TOC | 10701 ± 55 | 11950–12465 |
| 10445.1.1 | 65 | TOC | 13278 ± 53 | 15280–15620 |
| 9258.1.1 | 75 | TOC | 14885 ± 59 | 17450–17970 |
| 10446.1.1 | 85 | TOC | 15023 ± 37 | 17850–18160 |
| 9259.1.1 | 95 | TOC | 15663 ± 60 | 18310–18780 |
| 10447.1.1* | 113 | TOC | 12639 ± 51 | 14070–14800 |
| 9260.1.1 | 118 | TOC | 16840 ± 62 | 19620–20110 |
| 9261.1.1 | 138 | TOC | 19756 ± 69 | 23110–23740 |
| 10448.1.1* | 150 | TOC | 16553 ± 72 | 19390–19820 |
| 9262.1.1* | 158 | TOC | 35279 ± 164 | 39680–40500 |
| 10449.1.1* | 210 | TOC | 27453 ± 101 | 31060–31260 |
| 10450.1.1* | 256.5 | TOC | 37865 ± 301 | 41760–42340 |
| 9263.1.1* | 276.5 | TOC | 36221 ± 180 | 40640–41260 |
| 10451.1.1* | 302.5 | TOC | 35968 ± 241 | 40240–41200 |
| 10452.1.1 | 340.5 | TOC | 25704 ± 86 | 29300–29920 |
| 9264.1.1* | 362.5 | TOC | 37765 ± 295 | 41680–42320 |
| 10453.1.1 | 378.5 | TOC | 27410 ± 101 | 31060–31240 |
| 10454.1.1* | 428.5 | TOC | 29745 ± 124 | 33680–34300 |
| 9265.1.1* | 443.5 | TOC | 32142 ± 126 | 35820–36400 |
| 9266.1.1* | 483.5 | TOC | 39536 ± 361 | 42400–43020 |
| 10455.1.1* | 512.5 | TOC | 23440 ± 69 | 27240–27560 |
| 9267.1.1* | 560 | TOC | 37729 ± 211 | 41800–42240 |
| 10456.1.1 | 607 | TOC | 30982 ± 144 | 34660–35320 |
| 10457.1.1 | 675 | TOC | 29240 ± 120 | 33000–33800 |
| 9268.1.1* | 701.5 | TOC | 20975 ± 54 | 24650–25020 |
| 10458.1.1* | 733.5 | TOC | 28123 ± 107 | 31380–31920 |
| 9269.1.1* | 781.5 | TOC | 34949 ± 160 | 39340–40140 |
| 10459.1.1 | 820.5 | TOC | 30576 ± 138 | 34340–35040 |
| 10460.1.1 | 882.5 | TOC | 39806 ± 378 | 42440–43280 |
| 9270.1.1* | 910.5 | TOC | 28570 ± 91 | 31860–32860 |

(*continued on next page*)

**Table 1** (*continued*)

| Lab ID | Composite depth (cm) | Dated material | $^{14}$C age (yr BP) | Reservoir effect corrected and calibrated age (95% confidence interval; cal. yr BP) |
|---|---|---|---|---|
| 10461.1.1* | 940.5 | TOC | 29942 ± 127 | 33900–34420 |
| 9271.1.1 | 1000 | TOC | 38921 ± 235 | 42280–42660 |
| 9272.1.1 | 1020 | TOC | 37841 ± 298 | 41760–42340 |
| 9273.1.1 | 1060 | TOC | 39565 ± 255 | 42480–42940 |
| 9274.1.1 | 1080 | TOC | 37433 ± 203 | 41520–42120 |

compared to occurrences given by GBIF. Finally, the 'SibAla_2023' database includes a total of 4939 entries, comprising 3398 species, 947 genera, and 223 families that collapse into 2371 unique P6 loop sequence types (amplicon sequence variants, ASVs).

After running OBITools, we excluded the ASVs with less than 100% taxonomic identity. Non-metric multidimensional scaling (NMDS) analysis was subsequently performed via the *metaMDS* function in the R-package *vegan* (Oksanen et al., 2022) to check the PCR replicability of the samples and controls (Supplementary file S2). To estimate the taxonomic richness of terrestrial plants, the filtered data were subjected to rarefaction analysis (Birks and Line, 1992; the R code is available at https://doi.org/10.5281/zenodo.4562708) to a base count of 59,679 (i.e., the minimum count of a sample within the dataset). SedaDNA diagram (Fig. 5) was zoned by a qualitative inspection of significant changes in vegetation composition, occurrence of indicator taxa, and richness.

### 2.6. Statistical analyses

To statistically relate the variation in vegetation composition to summer and winter temperature changes, redundancy analysis (RDA) was implemented based on the Hellinger-transformed sedaDNA rarefied counts using the *RDA* function in the R-package *vegan* (Oksanen et al., 2022). RDA was chosen over canonical correspondence analysis because of the compositional gradient lengths of the sedaDNA data being <2.5 s.d. (standard deviation) as revealed by initial detrended correspondence analyses, indicating that linear-based ordination methods are appropriate with our dataset (Legendre and Birks, 2012). Considering that solar radiation is the primary forcing factor of temperature changes at orbital and suborbital scales (Bova et al., 2021; Laepple et al., 2011), mean summer and winter insolation at 63°N (Laskar et al., 2004) has been used as a proxy to assess summer and winter temperature variations. Due to the short spring and autumn seasons at high latitudes (Cooper, 2014), summer and winter insolation are indicated by warm-season (May to October) and cold-season (November to April) insolation, respectively, in the RDA model. To identify correlations between variables, Pearson's correlation analysis was run using the *cor* and *corr.test* functions in the R-package *psych* (Revelle, 2023). All statistical analyses were performed in RStudio (RStudio Team, 2020) with the R software (version 4.3.1; R Core Team, 2023).

## 3. Results

### 3.1. Core lithology and chronology

Based on lithological variations, sediment core EN21103 can be divided into two main parts. The upper part of the core (0−150 cm) is mainly composed of brown clay. The lower part (150−1100 cm) consists of discontinuous rhythmically laminated sediments that alternate between gray and greenish-gray/brown layers (Fig. 2B), which are similar to varve (Zolitschka et al., 2015). The total number of gray layers was visually counted to be approximately 380, suggesting that the lower parts of the core may not be continuously varved sediments.

The calibrated $^{14}$C ages lie in an overall steady sequence between 0 and 138 cm (Fig. 2A). However, there is not a good linear relationship between depths and calibrated $^{14}$C ages from 138 to 1100 cm, where most samples have been dated to MIS 3 and show age reversals. Based on the four dated samples between 1000 and 1080 cm, the age of the bottom of the core is estimated to be approximately 43 cal. ka BP. Given

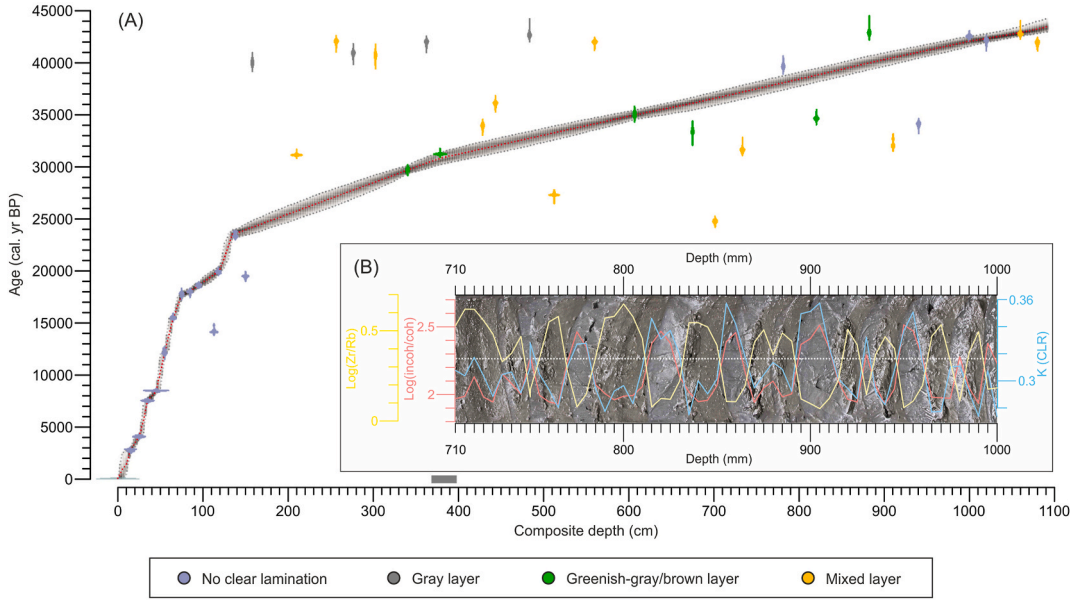


**Fig. 2.** (A) Bacon age-depth model constructed for core EN21103 from calibrated radiocarbon ages. Our data interpretation is insensitive to the age-depth model of 138–1100 cm, which was established based on the dating points that originated from pure greenish-gray/brown layer samples (green points) and four samples from the bottom of the core. The short gray band above the composite depth denotes the position of the sediment section shown in the plot B. (B) An example of rhythmical variations in the count of K (showing the same pattern as Ti, Al, Mg) and ratios of Zr/Rb and incoh/coh at 710−1000 mm in the sediment segment 'EN21103-3'. Compared to the greenish-gray layers, the gray layers have lower Zr/Rb ratios, higher incoh/coh ratios, and higher count of K. The dashed line denotes the position of XRF scanning detector.

the special lithological characteristics and the variability of other geochemical proxies from 150 to 1100 cm, the $^{14}C$ signal of gray layer samples may have been disturbed by older material from glacial activity, while the dating results of the greenish-gray/brown layer samples may be more reliable (see discussion in Section 4.1). The final age-depth model was established with a hiatus at 138 cm, and the model of 138–1100 cm was based on the dating points that originated from pure greenish-gray/brown layer samples and four samples with similar ages from the bottom of the core (Table 1 and Fig. 2). Our proxy data interpretation is insensitive to the age-depth model of 138–1100 cm (around 23.6−43 cal. ka BP). The average sedimentation rate of 0–138 cm and 138−1100 cm is 0.006 cm year$^{-1}$ and 0.048 cm year$^{-1}$, respectively.

### 3.2. Geochemical proxy records

TC and TOC results show broadly similar changes and vary between 0.458 and 6.003% (median 1.044%) and between 0.336 and 5.954% (median 0.921%), respectively (Fig. 3A and B). TC and TOC contents are relatively low (around 1%) and stable from 150 cm to the bottom and increase significantly in the upper 150 cm. A slight increase in TC and TOC contents is observed at 276.5−520 cm (around 27−33 cal. ka BP). Aside from some samples with undetectable values, the TN content (range 0.101–0.697%, median 0.138%) shows a similar pattern of variation as TC and TOC (Fig. 3C). TIC content is very low across the entire core, varying between 0.101 and 0.35% (median 0.141%, excluding undetectable values; Fig. 3E). Sedimentary organic matter in a lake generally originates from autochthonous and allochthonous sources, which can be distinguished by the ratio of TOC and TN (C/N). Lake Ulu generally has low C/N ratios (<10; Fig. 3F), suggesting that organic matter is mainly contributed by autochthonous input (Meyers, 2001). Fluctuations in $\delta^{13}C_{org}$ values (range −29.8 to −23.3‰, median −23.9‰) show a reverse trend to that of TC, TOC, and TN contents (Fig. 3D), where $\delta^{13}C_{org}$ values in the upper 150 cm (average −28.5‰) are relatively lighter than those in 150–1100 cm (average −23.9‰). This means that organic matter is still mainly derived from within the lake (e.g., algae), but may be more terrestrial-sourced in the upper part of the core, and that TOC content can be used as a proxy to reflect the primary organic productivity of the lake (Leng and Marshall, 2004; Liu et al., 2009; Meyers, 2001).

The incoherent/coherent (incoh/coh) ratio, an additional proxy for organic content (Croudace and Rothwell, 2015; Pedersen et al., 2016), shows a similar pattern of variation as TOC content ($R = 0.8$, $p < 0.001$, n = 72) and the Mn/Fe ratio ($R = 0.37$, $p < 0.001$, n = 2114; Fig. 4). The Zr/Rb ratio fluctuates more widely at 150−1100 cm and has a negative correlation with TOC contents ($R = -0.57$, $p < 0.001$, n = 72) and the incoh/coh ratio ($R = -0.30$, $p < 0.001$, n = 2114). Notably, rhythmical variations in the XRF scanning data are observed in the lower laminated

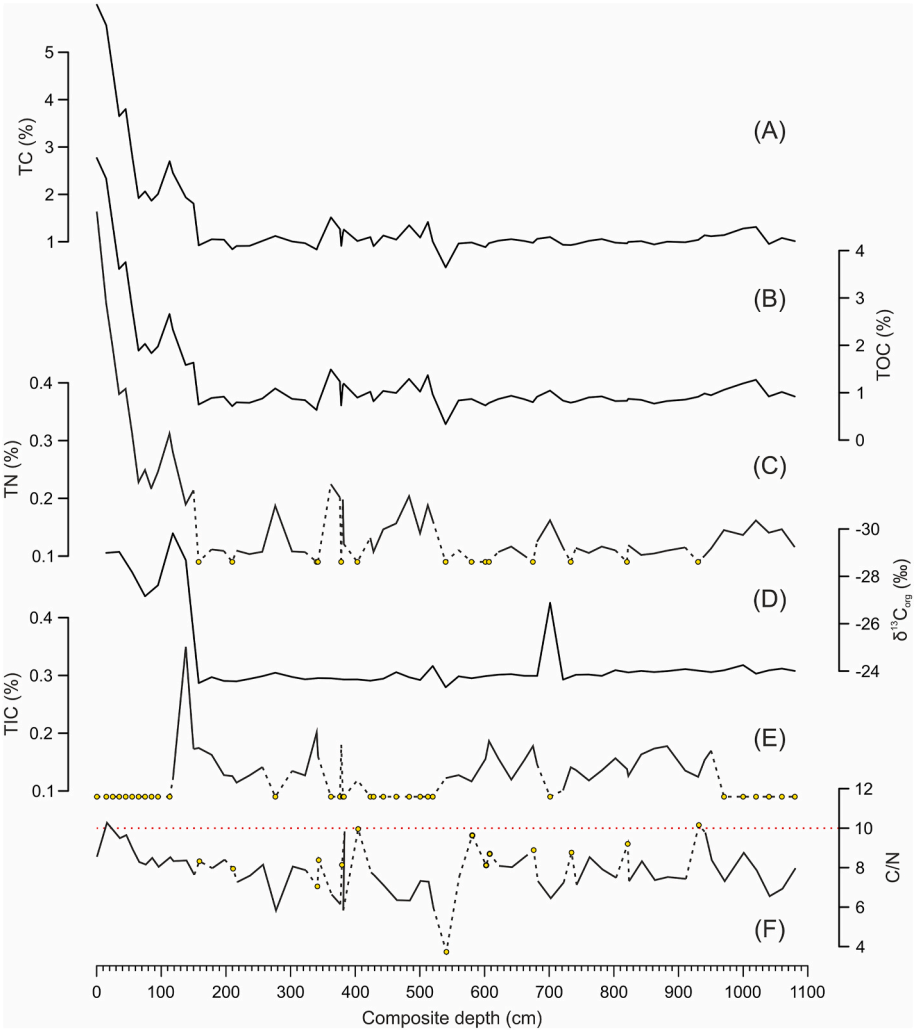


**Fig. 3.** (A) Total carbon (TC), (B) total organic carbon (TOC), (C) total nitrogen (TN), (D) organic carbon isotope ($\delta^{13}C_{org}$), (E) total inorganic carbon (TIC), and (F) the ratio of TOC and TN (C/N) variations versus composite depth of Lake Ulu. The yellow points denote undetectable values (<0.1%). TN values for these samples were replaced by 0.09 in the C/N calculation. The red dashed line denotes the ratio of C/N is equal to 10.

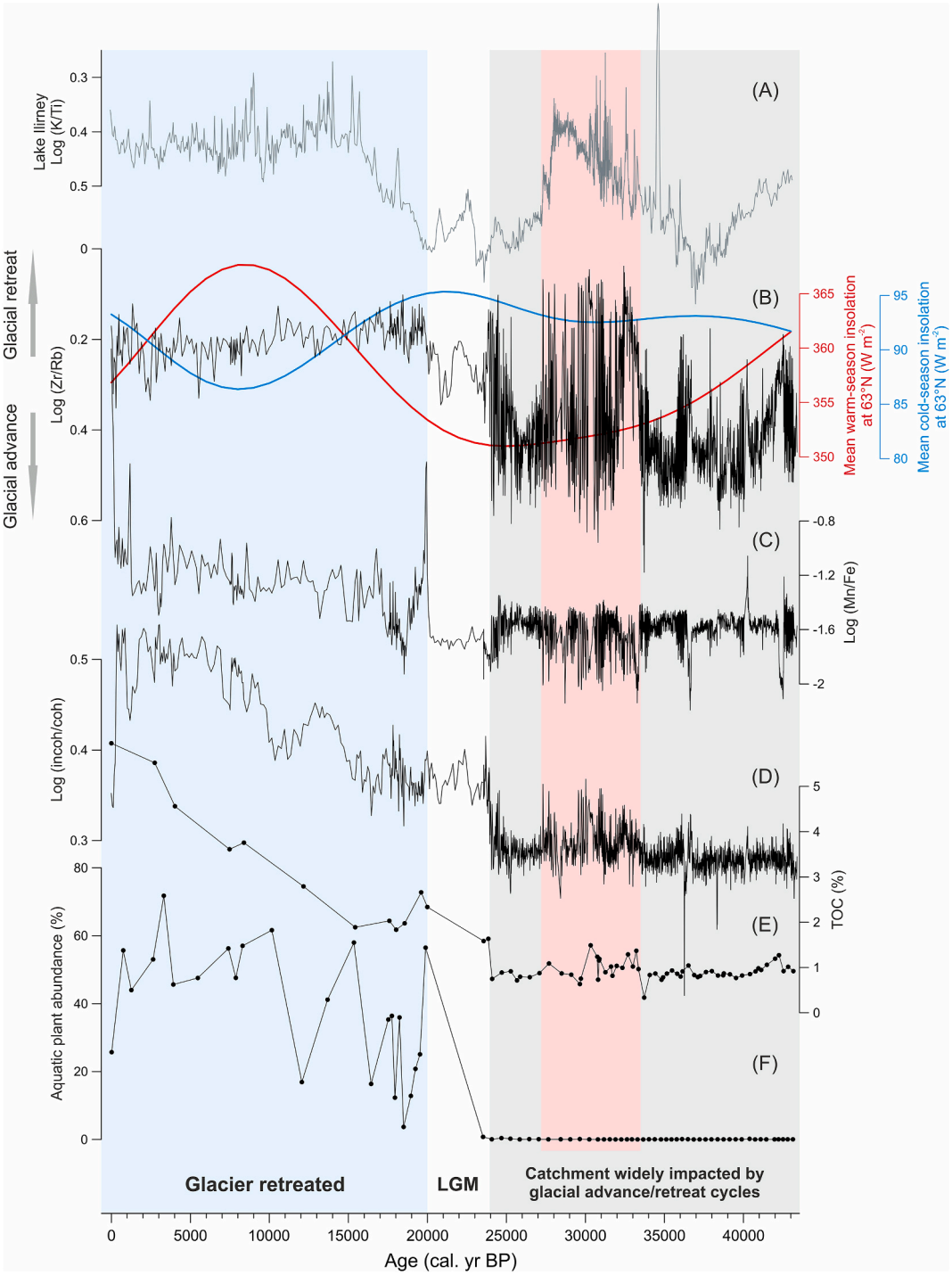


**Fig. 4.** (A) The K/Ti ratio of Lake Ilirney (Vyse et al., 2020). (B) Warm-season (red line) and cold-season (blue line) solar insolation at 63°N (Laskar et al., 2004). The records of Zr/Rb (B), Mn/Fe (C), incoh/coh (D), TOC (E), and aquatic plant abundance (F) from Lake Ulu. Glacial fluctuations indicated by the ratios of Zr/Rb (B). The vertical gray bar indicates the time period (around 43–23.6 cal. ka BP) when the lake catchment was widely impacted by glacial advance/retreat cycles. The vertical pink bar indicates a short warm period (around 33–27 cal. ka BP) and the white bar marks the LGM (around 23.6–20 cal. ka BP). The vertical light blue bar indicates when the catchment was glacier-free (around 20 cal. ka BP to the present).

sediments (approximately 150–1100 cm; Fig. 2B). Compared to the greenish-gray/brown layers, the gray layers have lower Zr/Rb ratios but higher incoh/coh ratios and higher counts of some rock-forming elements, such as K, Ti, Al, and Mg, which are positively intercorrelated ($R \geq 0.7$, $p < 0.001$, $n = 2114$) and typically sourced from terrigenous sediment input (Croudace and Rothwell, 2015; Larson et al., 2015).

### 3.3. Plant DNA metabarcoding

In total, 563 ASVs have 100% sequence similarity with the 'SibAla_2023' database. Of these, 440 sequences are assigned to terrestrial seed plant taxa, and 36.8% and 48.6% of them could be identified to genus and species level, respectively (Supplementary file S6). Thirty-one sequences are assigned to aquatic plant taxa, and 32.3% and 64.5% of them could be identified to genus and species level, respectively

(Supplementary file S6). NMDS results show high similarity in taxonomic composition among the three PCR replicates of each sample, except for slight variations in the top two samples (Supplementary file S2), and all controls were mostly free from any contamination. Sequence counts of DNA extraction controls and NTCs are 2% and 0.4% of the total counts, respectively.

Terrestrial plant compositional changes inferred from the sedaDNA record are clearly divided into two main zones (Fig. 5). Zone I (approximately 1100–138 cm, 43–23.6 cal. ka BP) is dominated by *Dryas*, *Papaver*, Saliceae, and Anthemideae. Higher percentages of some alpine and mountain plants such as *Oxyria digyna*, *Saxifraga*, *Draba*, and *Eritrichium* are also found. Trees and shrubs (e.g., *Populus*, *Alnus*, *Larix*, *Betula*) are present at very low percentages. The plant assemblages are relatively stable with few taxonomic shifts. Total and rarefied richness are also stable and at a high level. Zone II (approximately 138–0 cm, 23.6–0 cal. ka BP) is remarkable due to increased percentages of boreal trees and shrubs (e.g., *Larix*, *Betula*, *Rhododendron*, *Vaccinium*) along with a decline in richness. Such an unexpected pattern between richness and forest expansion has also been observed in the previous sedaDNA records (Courtin et al., 2021; Huang et al., 2021; Liu et al., 2021), which may be related to the loss of habitat and diversity of herbaceous plants, and needs to be evidenced by more studies in the future. Zone II can be further divided into three subzones. Zone IIa (approximately 138–103 cm, 23.6–19 cal. ka BP) is notable for its decreased percentages of *Dryas*, Saliceae, and other alpine and mountain plants. Conversely, percentages of Anthemideae and *Myosotis alpestris* reach their highest level throughout the core but decline quickly alongside a gradual increase in the percentage of Saliceae. There is a slight increase in the percentage of *Larix* and *Betula*, but they still remain at a low level. Zone IIb (approximately 103–53 cm, 19–11.3 cal. ka BP) shows a significant increase in the percentage of *Larix*, *Betula*, *Populus*, *Alnus*, and typical understory shrubs (e.g., *Rhododendron tomentosum*, *Vaccinium vitis-idaea*), while the percentages of *Dryas*, *Papaver*, and Anthemideae decreased. *Larix* expanded prior to *Betula* at approximately 18.6 cal. ka BP, whereas the latter expanded at approximately 17.8 cal. ka BP. A clear increase in the percentage of *Alnus alnobetula* is observed at approximately 15.4 cal. ka BP. Zone IIc (approximately 53–0 cm, 11.3–0 cal. ka BP) is notable for the further expansion of larch and understory shrubs, and the increased percentage of more wet- and shade-adapted herbaceous plants (e.g., *Ranunculus*, *Empetrum nigrum*).

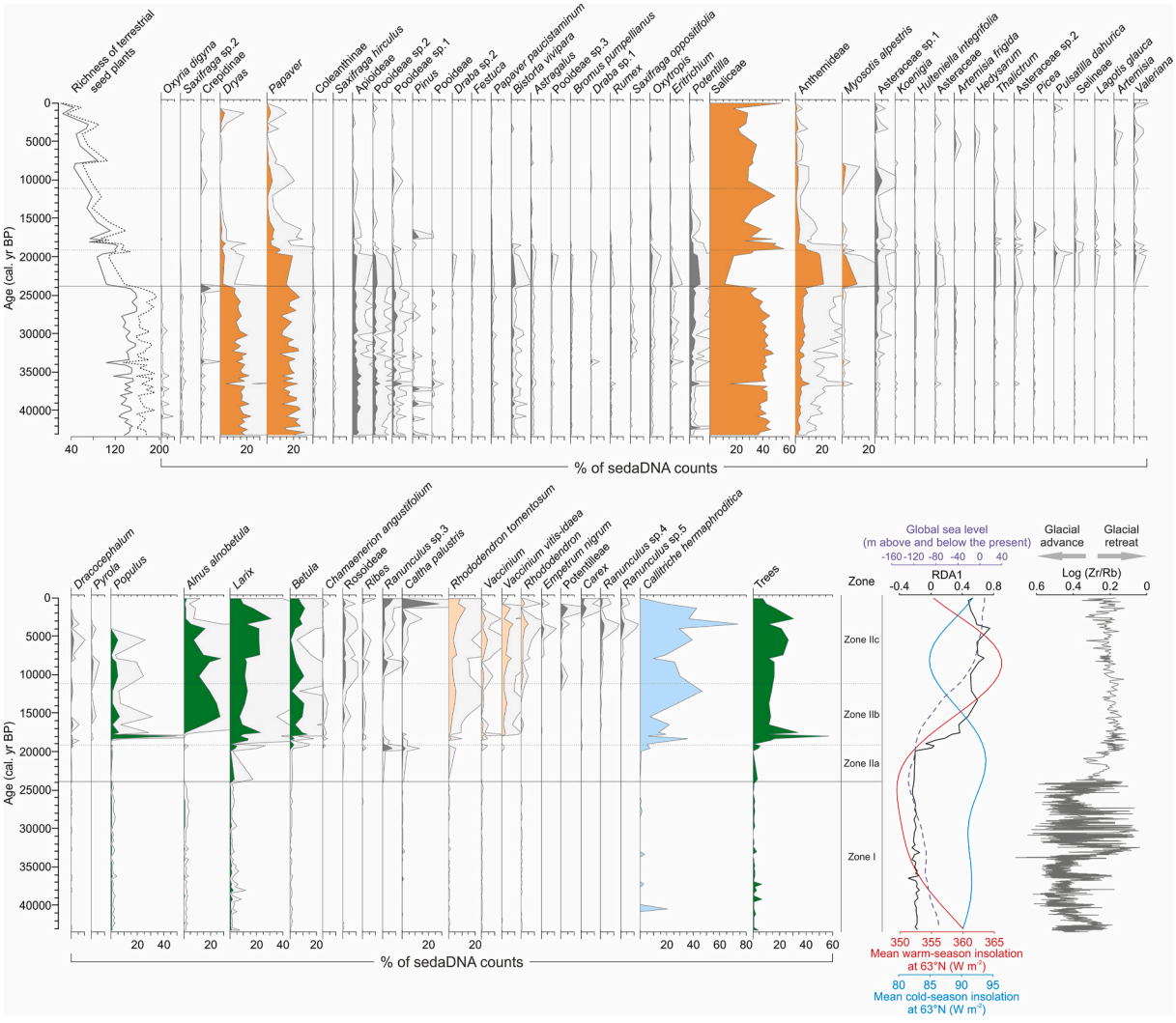


**Fig. 5.** Stratigraphic plot of sedimentary ancient DNA (sedaDNA) results with total richness (black dotted line) and rarefied richness (gray line) of terrestrial seed plant taxa and relative percentages of selected terrestrial plant taxa (with cumulative percentages >5%; shaded areas are 5 times exaggeration of scale), *Callitriche hermaphroditica* (aquatic plant), and trees in each sample. Two main sedaDNA zones and three subzones are shown. The second end panel shows the scores for the first axis of redundancy analysis (RDA1; black line) from Lake Ulu and compared with global sea level (purple dotted line; Spratt and Lisiecki, 2016) and warm-season (red line) and cold-season (blue line) solar insolation at 63°N (Laskar et al., 2004). The last panel shows the Zr/Rb record from Lake Ulu, which indicates glacial fluctuations.

Aquatic plant communities are dominated by Plantaginaceae (i.e., *Callitriche hermaphroditica*) and Potamogetonaceae. The proportion of aquatic plant counts to total vascular plant counts remains at a very low level but shows a sharp increase at approximately 20 cal. ka BP (Fig. 4F). A large expansion of *Callitriche hermaphroditica* is synchronous with that of *Larix* from approximately 18.6 cal. ka BP (Fig. 5).

### 3.4. Vegetation changes in relation to seasonal solar insolation

The first two RDA axes explain 31% of the variance in the terrestrial plant DNA data (Fig. 6). Warm-season and cold-season insolation independently explain 7.9% and 2.5% of the variation in terrestrial plant composition, respectively ($p < 0.001$; analysis of variance, ANOVA). A big shift from tundra-steppe assemblages dominated by *Dryas*, *Papaver*, and Anthemideae to boreal tree and shrub assemblages dominated by *Larix*, *Betula*, *Alnus alnobetula*, *Rhododendron tomentosum*, and *Vaccinium vitis-idaea* is observed at approximately 19 cal. ka BP, which is positively related to warm-season insolation and negatively related to cold-season insolation.

## 4. Discussion

### 4.1. Glacial activity and development of Lake Ulu

Coarse-grain sands and the calibrated radiocarbon age at the core bottom (Table 1 and Fig. 2) show that Lake Ulu was likely initiated by glacial retreat during MIS 3. The Oymyakon Upland was extensively influenced by glacial activities originating from the southern Suntar-Khayata Mountains (Barr and Clark, 2012; Lozhkin et al., 2018), resulting in a complex dendritic drainage pattern and a broad distribution of glacial deposits (Ministry for Natural Resources and Ecology of the Russian Federation, 2011, 2014). The ice limit of MIS 4 in the mountains to the north of Lake Ulu (Ministry for Natural Resources and Ecology of the Russian Federation, 2014) suggests that glacial dams formed during MIS 4 might have altered the flow direction of the ancient Kobyuma River, which had previously flowed eastward via today's Lakes Tschuch'ye and Ulu (Fig. 1B; Lozhkin et al., 2018), to now flow northwards, bypassing the Lake Ulu catchment.

The Zr/Rb ratio can be used as a proxy for glacial fluctuations in the Lake Ulu catchment. Zr is enriched in heavy minerals and medium-to-coarse silts and sands (Dypvik and Harris, 2001). Rb, being chemically similar to K, is abundant in clay minerals dominated by fine-grained siliciclastic material (Biskaborn et al., 2013; Liu et al., 2014). In general, glacial advance can enhance bedrock erosion that leads to

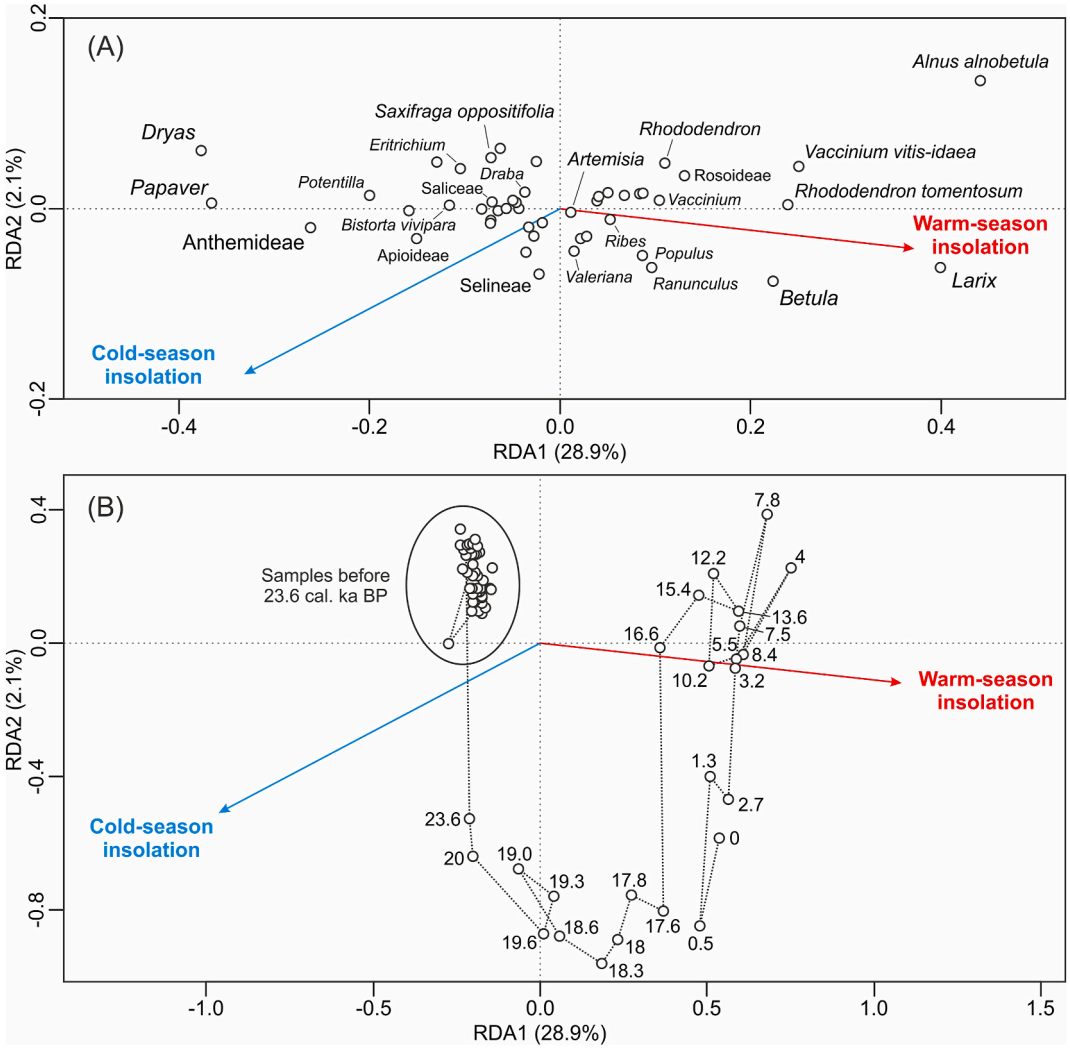


**Fig. 6.** Redundancy analysis (RDA) showing the influence of warm-season (red line) and cold-season (blue line) solar insolation at 63°N on the composition of all terrestrial plant taxa (A) and on age (unit: cal. ka BP) trajectories (B). Only dominant taxa (with relative percentages >1%) are marked in the biplot A.

increased transport of coarse-grained clastic material and eventually Zr input into the lake. In contrast, during glacial retreat, Rb that attaches to fine-grained particles could be transported into the lake by glaciofluvial runoff when the catchment experiences a lower erosion rate. Accordingly, the Zr/Rb ratio is considered a proxy for glacial fluctuations with high ratios indicating glacial advance and vice versa (Liu et al., 2014). This is further verified by the good correlation between the Zr/Rb ratio of Lake Ulu and the K/Ti ratio of Lake Ilirney from Chukotka over the last 43 cal. ka BP ($R = 0.45$, $p < 0.001$, n = 4335; Fig. 1A and 4A), which was used as a proxy for physical weathering associated with glacial fluctuations (Vyse et al., 2020). In addition, the ability of the Zr/Rb ratio to represent glacial activity is supported by its rhythmical variation in the lower laminated sediments of Lake Ulu (around 150−1100 cm). Gray layers exhibit lower Zr/Rb ratios, higher incoh/coh ratios (indicating organic matter), and higher counts of rock-forming elements such as K, Ti, Al, and Mg (Fig. 2B). These characteristics may have formed during glacial retreat when more fine-grained and terrigenous materials would have been carried into the lake by increased fluvial runoff, resulting in an increase in lake organic productivity. Under this concept, glacial advance is reflected by increased transport of coarse-grained clastic materials (higher Zr/Rb ratios), decreased lake organic productivity (lower incoh/coh ratios), and weaker development of catchment runoff (lower counts of K, Ti, Al, Mg) in the greenish-gray/brown layers. Our hypothesis is further supported by elemental measurements of two defined gray layers and one intermediate greenish-gray layer in the core section between 376 and 381.5 cm (Supplementary file S3). The two gray layers have higher TOC contents and C/N ratios than the greenish-gray layer between them, while the opposite pattern is observed for TIC. Larger catchment areas and stronger runoff during glacial retreat likely carried old carbon into the lake and mixed it with carbon originating from in-situ bioproduction in younger sediments, thus interfering with the $^{14}C$ signal. Hence, we speculate that the radiocarbon dating results in the lower part of the core may have been affected by glacial advance/retreat cycles in the catchment area, and the $^{14}C$ dating results of samples from the greenish-gray/brown layers are more likely to represent reliable age estimates. Based on this concept, only the dating points from pure greenish-gray/brown layer samples and four samples with similar ages from the bottom of the core were considered for the age-depth calculation (Table 1 and Fig. 2A). Nevertheless, such varve-like sediments from the lower part of the core need to be further studied by, for example, optical microscope analyses to obtain a better sedimentological archive in the future.

The development of Lake Ulu since the middle of MIS 3 has been strongly influenced by glacial activity, which is primarily driven by variations in summer solar insolation. According to the Zr/Rb record, the lake catchment was likely covered by extensive glaciers and ice sheets for a long time and experienced multiple glacial advances and retreats between 43 and 23.6 cal. ka BP, which generally followed low warm-season insolation at 63°N (Fig. 4B; Laskar et al., 2004). Due to cold climatic conditions, lake organic productivity was low, leading to relatively low TOC contents (and incoh/coh ratios) during this time (Fig. 4D and E), accompanied by long and possibly semi-permanent lake ice cover. Large parts of the soil were covered by widespread glaciers and ice sheets, limiting the development of vegetation and allowing the catchment to maintain a stable tundra-steppe landscape dominated by *Dryas*, *Papaver*, Saliceae, and Anthemideae (Fig. 5). The presence of glaciers is also indicated by low Mn/Fe ratios during this period (Fig. 4C), which suggests that the lake and its catchment were poorly ventilated, leading to anoxic conditions in the sediment, as Mn is more easily reduced than Fe under anoxic conditions (Naeher et al., 2013; Vyse et al., 2020). A short and discontinuous period of glacial retreat is inferred at approximately 33−27 cal. ka BP, when the Zr/Rb ratios are relatively high but frequently fluctuate, indicating that the glacier has not fully retreated from the catchment, as is also evidenced by consistently low Mn/Fe ratios. In addition, an increase in lake organic productivity, as reflected by higher TOC contents and incoh/coh ratios, implies a possible warm scenario, which has also been reported in previous records from Siberia (Lake Ilirney, Vyse et al., 2020, Fig. 4A) and Alaska (Lapointe E. et al., 2017). The agreement of this short-term event with other studies further evidences the usability of the age-depth model we have established. A glacial retreat, marked by a pronounced reduction in the Zr/Rb ratio, is inferred to have occurred at approximately 23.6−20 cal. ka BP, following an increase in mean warm-season insolation. Such a transition is also indicated by a gradual increase in lake organic productivity (TOC contents and incoh/coh ratios) and an obvious lithological change (i.e., a shift from laminated sediments to brown clay at 150 cm), suggesting a possible shift in the primary sediment source from coarse-grained glacial clastic material to fine-grained and organic-rich particles. This time period is considered the LGM, when the region experienced extremely low precipitation and snowfall (Clark et al., 2009), resulting in severe aridity and a decline in glacial volume in the lake catchment. The widespread lack of glaciation in the nearby Verkhoyansk Mountains during the LGM is thought to be due to insufficient moisture supply (Barr and Clark, 2012), as the Westerlies from the North Atlantic Ocean were restricted by vast ice sheets (Gowan et al., 2021). This drought event is also reflected in our sedaDNA record by a significant decrease in the percentage of *Dryas* and Saliceae, accompanied by elevated percentages of *Papaver*, Anthemideae (Asteraceae; Folk et al., 2020), and *Myosotis alpestris* (Schuchardt et al., 2021); plants that are more adapted to cold and drought. In addition, the continentality of the Oymyakon region was likely to be maximized during the LGM, which was coincident with the lowest global sea level (Fig. 5; Spratt and Lisiecki, 2016) and the largest ice volume in the Northern Hemisphere (Gowan et al., 2021), possibly resulting in even faster summer warming. We infer that the glacier fully retreated and reached its present volume at approximately 20 cal. ka BP, which is when the Zr/Rb ratio shows a further decrease and reaches a relatively stable plateau. The Mn/Fe ratios reach a peak at the same time, which suggests notable increases in lake ventilation due to the longer ice-free period. This is also evidenced by the expansion of aquatic plants starting at approximately 20 cal. ka BP in our sedaDNA record (Fig. 4F), which may be caused by increased summer temperature and lake water conductivity via fluvial runoff (Stoof-Leichsenring et al., 2022). A distinct glacial retreat at around 20 cal. ka BP has also been reported in other records from eastern Siberia (e.g., Margold et al., 2016; Lake Ilirney, Vyse et al., 2020) and Alaska (e.g., Briner and Kaufman, 2008; Elias and Brigham-Grette, 2013), implying a regional-scale response of glacier volumes to temperature and moisture changes. The ice-cover period of the lake was further shortened after 20 cal. ka BP, as shown by a fast increase in Mn/Fe ratios and aquatic plant abundance, which may be related to more extensive glacial retreat and summer warming (Stoof-Leichsenring et al., 2022).

### 4.2. *Vegetation dynamics in response to summer and winter temperature changes*

Overall, we infer from our analyses of the sedaDNA record that long-term vegetation dynamics since the middle of MIS 3 were highly sensitive to summer rather than winter temperature changes, even in the Oymyakon region - one of the coldest areas of the Northern Hemisphere. To our knowledge, this is the first sedaDNA record from the Oymyakon region, with most of the previous studies on vegetation changes being based on pollen and macrofossil records (e.g., Anderson et al., 2002; Binney et al., 2009; Lozhkin et al., 2018).

We expect that vegetation dynamics in the Oymyakon region might be more sensitive to changes in winter rather than summer temperatures, because this area has been subjected to extremely cold winters and continental conditions, especially during the LGM, when the global sea level reached its lowest level in the last 43 ka BP (Fig. 5; Spratt and Lisiecki, 2016) and the Arctic coast was estimated to have been located approximately 600–900 km to the north of the present-day coastline (Fig. 1A; Anderson and Lozhkin, 2015). However, this assumption is not supported by our records. The sedaDNA results reveal that a

tundra-steppe landscape occurred during most of the time and started to collapse at the end of the LGM (around 19 cal. ka BP) following the expansion of trees and shrubs (Fig. 5), which corresponds to the timing of the glacial retreat and increased warm-season insolation. Such a big shift in terrestrial plant functional groups was not noted at approximately 23.6–19 cal. ka BP, when cold-season insolation reached its highest level over the past 43 cal. ka BP. Likewise, RDA results suggest that the vegetation shift from tundra-steppe assemblages dominated by *Dryas*, *Papaver*, and Anthemideae (cold-adapted plants) to boreal tree and shrub assemblages dominated by *Larix*, *Betula*, *Alnus*, *Rhododendron*, and *Vaccinium* (warm-preferring plants) is positively related to variations in warm-season rather than cold-season insolation (Fig. 6). Variations in the score of RDA axis-1 are highly positively consistent with those of warm-season insolation (Fig. 5; $R = 0.74$, $p < 0.001$, n = 71). Sensitivity of vegetation dynamics to summer warming is also reflected in specific plant taxa. For example, green alder (*Alnus alnobetula*), whose growth is highly sensitive to temperature and light (Drew et al., 2023; Oberhuber et al., 2022), was abundant at approximately 15.4–13.6 cal. ka BP, indicating significant climate warming. Such warming is most likely caused by an increase in warm-season insolation rather than cold-season insolation, which actually decreased over this period. Alder abundance began to decline from about 4 cal. ka BP following the summer cooling of the late Holocene. The large expansion of *Larix* at approximately 18.6 cal. ka BP is synchronous with that of *Callitriche hermaphroditica*, which is regarded as a good indicator of mean July temperatures above 12 °C (Kienast et al., 2005). Similarly, the reduction in *Bistorta vivipara* after approximately 18.6 cal. ka BP may be due to increased summer temperatures. As *Bistorta vivipara* has a fixed growth period, summer warming can advance, but not prolong, its growth period, making it less able to compete with other warm-season species (Cooper, 2014; Starr et al., 2001).

We interpret the higher sensitivity of postglacial plant assemblages to summer temperature changes as mainly relating to (i) significant differences in the amplitudes between summer and winter insolation; (ii) the strong continentality of the Oymyakon region; and (iii) the lengthening of the plant growing season. The amplitude of warm-season insolation (16.67 W $m^{-2}$) is much higher than that of cold-season insolation (8.98 W $m^{-2}$) over the past 43 ka BP (Fig. 5), leading to the strong dominance of summer insolation in the variability of annual insolation and a highly consistent trend between summer and annual insolation ($R = 0.95$, $p < 0.001$, n = 44). Between about 23 and 18 ka BP, the increase in warm-season insolation of about 4.65 W $m^{-2}$ dominated over the cold-season insolation decrease of about 0.79 W $m^{-2}$. Significant seasonality driven by such orbital forcing would result in higher temperature amplitudes between summer and winter months during the postglacial period, resulting in fast summer warming. The magnitude of this summer warming is likely to be even greater in the Oymyakon region due to the amplification of extreme continentality. On the other hand, an increase in summer temperature can result in an earlier spring snowmelt and a later winter snowfall, which lengthens plant growing season and thus advances plant phenological events. These processes can increase plant production and shape community structure (Ernakovich et al., 2014; Piao et al., 2019). Because variations in warm-season insolation far dominate over cold-season insolation, an extended growing season from increased summer temperatures may outweigh the negative effects of decreased winter temperatures after the LGM.

Regional plants, such as *Larix* (Bondar et al., 2022), *Populus*, *Betula* (Chang et al., 2021), *Ranunculus*, and Poaceae (Gupta and Deswal, 2014), generally carry cold adaptive genes and secrete antifreeze proteins (Griffith and Yaish, 2004; Wisniewski et al., 2020), which allow them to survive even in extremely harsh winters. For example, the primary regulators of the transcriptional cold response network in higher plants are the *CBF/DREB1* (C-repeat Binding Factor/Dehydration-Responsive Element-Binding protein 1) gene family, which are widely homologous in woody angiosperms such as poplar and birch (Chang et al., 2021). These cold responsive processes could genetically make plants less sensitive to winter temperature changes.

### 4.3. Potential glacial refugia and early postglacial expansion of larch

Unexpected early expansion of *Larix* after the LGM (approximately 18.6 cal. ka BP) in eastern Siberia has been uncovered by the sedaDNA record from Lake Ulu. Pollen record from Lake Smorodinovoye (Fig. 1A), also located in the Upper Indigirka Basin and 160 km north of Lake Ulu, show that the first postglacial appearance of *Larix* was at approximately 9.6 $^{14}$C ka BP (Anderson et al., 2002). Hybridization capture of chloroplast and nuclear genomes and pollen results from Lake Emanda (Fig. 1A; 330 km northwest of Lake Ulu) reveal that the expansion of *Larix* started around 13–9 cal. ka BP (Schulte et al., 2022b). Other macrofossil and pollen records from eastern Siberia also suggest that the first occurrence of *Larix* was not earlier than 17 ka BP, and that larch forests grew across much of eastern Siberia until the beginning of the Holocene (Binney et al., 2009; Brubaker et al., 2005; Herzschuh et al., 2022; Lozhkin et al., 2018; Schulte et al., 2022b). We also notice that *Larix* pollen has been detected in a few records from eastern Siberia during the LGM, but either at very low abundances (<0.5%) or in rivers or streams, where the pollen may have been transported over long distances (e.g., Kirgirlakh Stream in the basin of Berelyekh River; Anderson and Lozhkin, 2002). Hence, our sedaDNA record show the possibility that larch survived within glacial refugia in the catchment of Lake Ulu and expanded quickly *in situ* after the LGM, rather than migrated from other regions.

Our assumption that the existence of glacial refugia is supported by several results. First, if larch migrated from other regions, its first appearance and expansion should lag climate change by some time, because of dispersal rates and migration distances. However, if larch survived in local refugia, its first population increase could be nearly contemporaneous with the onset of climate warming (Brubaker et al., 2005). There is a slight increase in the percentage of *Larix* at approximately 23.6–19 cal. ka BP, which basically fits the initiation of glacial retreat and increased warm-season insolation (Fig. 5). In addition, *Callitriche hermaphroditica* is a reliable indicator of mean July temperatures higher than 12 °C (Kienast et al., 2005), which coincides with the ideal summer growing temperature for *Larix*, especially for *Larix cajanderi* (Schulte et al., 2022a). Their simultaneous expansion at approximately 18.6 cal. ka BP further suggests the existence of local refugia for larch. Second, *Larix*'s DNA is detectable across the entire core with high PCR repeatability (213 occurrences in 213 PCR replicates), even before 23.6 cal. ka BP (at a low percentage), which differs from other tree taxa and has been further supported by our metagenomic results (unpublished data). This means that small patches of larch forest have always survived locally, even during the period when the catchment area was widely impacted by mountain glaciers. Third, the expansion of *Betula* lagged that of *Larix* by approximately 800–1000 years, which is an uncommon phenomenon because *Betula* is an early-successional pioneer taxon in the plant community (Jonczak et al., 2020). This also suggests that larch forests probably expanded *in situ* rather than from external migration. Larch can survive in harsh environments with a dwarfing growth mode and other morphological strategies (Kruse et al., 2020). *Larix cajanderi* is the most widespread species in the modern lake catchment and the most cold- and drought-tolerant species in the genus *Larix*. More importantly, this species can grow even on recently disturbed and poorly drained soils, for example, on extensive continuous permafrost with a very low active layer thickness (<1 m; Schulte et al., 2022a), which impedes the development of evergreen forests (Herzschuh et al., 2016). Fire has been considered as another factor to promote postglacial colonization of larch forests because they are morphologically and physiologically more resistant to frequent fire events in Siberia than evergreen trees (e.g., *Abies* and *Picea*; Schulte et al., 2022a; Schulze et al., 2012). Herzschuh (2020) also points out that larch had higher genetic diversity than evergreen taxa during the glacial period as they can exchange genetic information over long distances, which may give them more flexibility

to respond to postglacial warming. All these characteristics enable larch to quickly colonize poorly developed soils on the permafrost without competitors and to pioneer the establishment of deciduous boreal tree and shrub communities during the post-LGM warming.

Glacial refugia in the Oymyakon region were unexpected and previously unnoticed, which challenges the current views on refugial locations. Potential refugia could also explain the surprisingly high number of ASVs (i.e., 563 ASVs with 100% identity) found in our metabarcoding data, which exceeds that of previous plant DNA metabarcoding studies from Siberia (e.g., Clarke et al., 2019; Courtin et al., 2021; Huang et al., 2021; von Hippel et al., 2022). Mountainous regions have long been argued as hotspots of glacial refugia for cold-adapted and alpine plants, as continued moisture availability and complex topography offers a variety of microclimatic conditions and suitable habitats (Dobrowski, 2011; Schönswetter et al., 2005; Stewart et al., 2010). We hypothesize that the putative refugia might be located in the deep valleys of the northern mountains that dammed the advance of glaciers from the southern Suntar-Khayata Mountains and possibly became a glacier-free area (Lozhkin et al., 2018). Today, dense larch forest can still be found in these places, and their DNA could probably be transported over shorter distances to the lake via mountain streams. The absence of glacial refugia around Lake Smorodinovoye and Lake Emanda may thus be explained by their relatively flat and homogenous catchment areas (Baumer et al., 2021). From this perspective, it is promising that more refugia might be found in the mountain ranges of the Oymyakon region and southern Yakutia, which requires more studies in the future.

Our results imply that the past distribution of *Larix* and refugia may be underestimated in eastern Siberia, and the Oymyakon region may be one of the earliest sources for larch postglacial recolonization, which provides a new insight into the distances and rates of plant expansion and migration after the LGM. It is now realized that northern refugia have played a crucial role in the postglacial reforestation of Eurasia (Feurdean et al., 2013; Stewart et al., 2010), especially for larch forests (Herzschuh, 2020; Schulte et al., 2022a), but less attention has been paid to highland areas in general, and southern Yakutia in particular. To better predict future scenarios of Siberian larch forest responses to global warming, more systematic paleoecological studies based on sedaDNA analysis are proposed to produce more reliable estimates of past species ranges and their dispersal rates that can be applied in simulation models. Given the current fast warming in conjunction with permafrost thaw (Biskaborn et al., 2019) and frequent wildfires in Siberia (Ponomarev et al., 2016), we speculate that the dominance of larch forest will remain stable in the short term but their further expansion will likely be constrained by limited moisture availability (Berner et al., 2013).

## 5. Conclusions

Based on the geochemical and sedaDNA records from the sediment core of Lake Ulu covering the last 43 cal. ka BP, we draw the following conclusions.

(i) Lake Ulu was likely initiated by glacial retreat during MIS 3. The Zr/Rb ratio can be used as a proxy for glacial activity in the lake catchment, which is primarily forced by variations in summer solar insolation. The catchment area has experienced multiple glacial advance/retreat cycles between 43 and 23.6 cal. ka BP, which limits vegetation development. The glacier retreated extensively from around 23.6 cal. ka BP and fully retreated from the catchment at around 20 cal. ka BP.

(ii) Postglacial vegetation shifts from tundra-steppe assemblages to boreal tree and shrub assemblages were highly sensitive to summer rather than winter temperature changes, even in the Oymyakon region - one of the coldest areas of the Northern Hemisphere. This may be attributed to 1) the amplitude of summer insolation dominating over that of winter insolation; 2) the amplification of summer warming because of the extreme continentality of the Oymyakon region; and 3) the extension of the plant growing season. Cold adaptation of regional plants at the genetic level could be another important reason to consider.

(iii) Our sedaDNA record show the earliest postglacial expansion of larch in eastern Siberia (around 18.6 cal. ka BP) to date, which is possibly related to the existence of local glacial refugia. This implies that the past distribution of *Larix* and refugia in eastern Siberia may be underestimated, and the Oymyakon region may be one of the earliest sources for postglacial larch recolonization. Further sedaDNA studies should focus more on the mountainous region of southern Yakutia to provide a fuller picture of larch expansion and migration and to help predict future dynamics of Siberian larch forest under the changing climate.

## Author contributions

U.H. designed the study. B.K.B. led the retrieval of lake sediment cores. W.J. performed the laboratory work (guided by B.K.B., K.R.S.-L., U.H.). W.J. ran the data analyses and wrote the first draft of the manuscript (supervised by U.H.). All co-authors reviewed and edited the final manuscript.

## Declaration of competing interest

The authors declare that they have no known competing financial interests or personal relationships that could have appeared to influence the work reported in this paper.

## Data availability

DNA sequence data have been deposited in the European Nucleotide Archive (ENA) under accession number PRJEB70434 (https://www.ebi.ac.uk/ena/browser/view/PRJEB70434), using the data brokerage service of the German Federation for Biological Data (GFBio; Diepenbroek et al., 2014). The tag file needed to identify the samples in the two libraries and the script for running the OBITools 3 bioinformatic pipeline (Boyer et al., 2016) are given in Supplementary files S4 and S5, respectively. Geochemical data are available at the Pangaea (https://doi.pangaea.de/10.1594/PANGAEA.965485).

## Acknowledgments

We would like to express our gratitude to the editor Dr. Yan Zhao and two anonymous reviewers in strengthening this paper with their valuable feedback. We are grateful to Jan Kahl, Igor Syrovatskiy, and Philip Meister for their support during field work, and Holly E. L. Blevins, Antonia Eichner, Ramesh Glückler, Ying Liu, and Laura Schild for supporting us with the sediment core opening and subsampling. Modern vegetation survey data around Lake Ulu were provided by Stefan Kruse. Justin Lindemann, Antonia Eichner, Mikaela Weiner, and Hanno Meyer contributed to elemental and $\delta^{13}C_{org}$ analysis. Janine Klimke and Sarah Olischläger are thanked for their help with the ancient DNA laboratory work. Weihan Jia thanks Andrei A. Andreev, Stefan Kruse, Xingqi Liu, and Chenzhi Li for their helpful discussion. We also acknowledge Cathy Jenks for the English language editing. This study was funded by the European Research Council (Glacial*Legacy*; Grant No. 772852, Ulrike Herzschuh) and the China Scholarship Council (Grant No. 202008110205, Weihan Jia).

## Appendix A. Supplementary data

Supplementary data to this article can be found online at https://doi.org/10.1016/j.quascirev.2024.108650.

## References


Alsos, I.G., Lammers, Y., Yoccoz, N.G., Jørgensen, T., Sjögren, P., Gielly, L., Edwards, M. E., 2018. Plant DNA metabarcoding of lake sediments: how does it represent the contemporary vegetation. PLoS One 13, e0195403. https://doi.org/10.1371/journal.pone.0195403.

Alsos, I.G., Rijal, D.P., Ehrich, D., Karger, D.N., Yoccoz, N.G., Heintzman, P.D., Brown, A. G., Lammers, Y., Pellissier, L., Alm, T., Bråthen, K.A., Coissac, E., Merkel, M.K.F., Alberti, A., Denoeud, F., Bakke, J., PhyloNorway Consortium, 2022. Postglacial species arrival and diversity buildup of northern ecosystems took millennia. Sci. Adv. 8, eabo7434 https://doi.org/10.1126/sciadv.abo7434.

Anderson, P.M., Lozhkin, A.V., 2002. Late quaternary vegetation and climate of Siberia and the Russian far east (palynological and radiocarbon database). North East Science Center, Far East Branch. Russian Academy of Sciences, Magadan, Russia (in Russian).

Anderson, P.M., Lozhkin, A.V., 2015. Late quaternary vegetation of chukotka (northeast Russia), implications for glacial and Holocene environments of beringia. Quat. Sci. Rev. 107, 112–128. https://doi.org/10.1016/j.quascirev.2014.10.016.

Anderson, P.M., Lozhkin, A.V., Brubaker, L.B., 2002. Implications of a 24,000-yr palynological record for a Younger Dryas cooling and for boreal forest development in Northeastern Siberia. Quat. Res. 57, 325–333. https://doi.org/10.1006/qres.2002.2321.

Assis, J., Tyberghein, L., Bosch, S., Verbruggen, H., Serrão, E.A., De Clerck, O., 2018. Bio-ORACLE v2.0: extending marine data layers for bioclimatic modelling. Global Ecol. Biogeogr. 27, 277–284. https://doi.org/10.1111/geb.12693.

Baisheva, I., Pestryakova, L., Levina, S., Glückler, R., Biskaborn, B.K., Vyse, S.A., Heim, B., Herzschuh, U., Stoof-Leichsenring, K.R., 2023. Permafrost-thaw lake development in Central Yakutia: sedimentary ancient DNA and element analyses from a Holocene sediment record. J. Paleolimnol. 70, 95–112. https://doi.org/10.1007/s10933-023-00285-w.

Barr, I.D., Clark, C.D., 2012. Late Quaternary glaciations in Far NE Russia; combining moraines, topography and chronology to assess regional and global glaciation synchrony. Quat. Sci. Rev. 53, 72–87. https://doi.org/10.1016/j.quascirev.2012.08.004.

Baumer, M.M., Wagner, B., Meyer, H., Leicher, N., Lenz, M., Fedorov, G., Pestryakova, L. A., Melles, M., 2021. Climatic and environmental changes in the Yana Highlands of north-eastern Siberia over the last *c.* 57 000 years, derived from a sediment core from Lake Emanda. Boreas 50, 114–133. https://doi.org/10.1111/bor.12476.

Berner, L.T., Beck, P.S.A., Bunn, A.G., Goetz, S.J., 2013. Plant response to climate change along the forest-tundra ecotone in northeastern Siberia. Global Change Biol. 19, 3449–3462. https://doi.org/10.1111/gcb.12304.

Berner, L.T., Massey, R., Jantz, P., Forbes, B.C., Macias-Fauria, M., Myers-Smith, I., Kumpula, T., Gauthier, G., Andreu-Hayles, L., Gaglioti, B.V., Burns, P., Zetterberg, P., D'Arrigo, R., Goetz, S.J., 2020. Summer warming explains widespread but not uniform greening in the Arctic tundra biome. Nat. Commun. 11, 4621. https://doi.org/10.1038/s41467-020-18479-5.

Binney, H.A., Willis, K.J., Edwards, M.E., Bhagwat, S.A., Anderson, P.M., Andreev, A.A., Blaauw, M., Damblon, F., Haesaerts, P., Kienast, F., Kremenetski, K.V., Krivonogov, S.K., Lozhkin, A.V., MacDonald, G.M., Novenko, E.Y., Oksanen, P., Sapelko, T.V., Väliranta, M., Vazhenina, L., 2009. The distribution of late-Quaternary woody taxa in northern Eurasia: evidence from a new macrofossil database. Quat. Sci. Rev. 28, 2445–2464. https://doi.org/10.1016/j.quascirev.2009.04.016.

Birks, H.J.B., Line, J.M., 1992. The use of rarefaction analysis for estimating palynological richness from Quaternary pollen-analytical data. Holocene 2, 1–10. https://doi.org/10.1177/095968369200200101.

Biskaborn, B.K., Herzschuh, U., Bolshiyanov, D.Y., Schwamborn, G., Diekmann, B., 2013. Thermokarst processes and depositional events in a tundra lake, northeastern Siberia. Permafr. Periglac. Process. 24, 160–174. https://doi.org/10.1002/ppp.1769.

Biskaborn, B.K., Smith, S.L., Noetzli, J., Matthes, H., Vieira, G., Streletskiy, D.A., Schoeneich, P., Romanovsky, V.E., Lewkowicz, A.G., Abramov, A., Allard, M., Boike, J., Cable, W.L., Christiansen, H.H., Delaloye, R., Diekmann, B., Drozdov, D., Etzelmüller, B., Grosse, G., Guglielmin, M., Ingeman-Nielsen, T., Isaksen, K., Ishikawa, M., Johansson, M., Johannsson, H., Joo, A., Kaverin, D., Kholodov, A., Konstantinov, P., Kröger, T., Lambiel, C., Lanckman, J., Luo, D., Malkova, G., Meiklejohn, I., Moskalenko, N., Oliva, M., Phillips, M., Ramos, M., Sannel, A.B.K., Sergeev, D., Seybold, C., Skryabin, P., Vasiliev, A., Wu, Q., Yoshikawa, K., Zheleznyak, M., Lantuit, H., 2019. Permafrost is warming at a global scale. Nat. Commun. 10, 264. https://doi.org/10.1038/s41467-018-08240-4.

Blaauw, M., Christen, J.A., 2011. Flexible paleoclimate age-depth models using an autoregressive gamma process. Bayesian Anal 6, 457–474. https://doi.org/10.1214/11-BA618.

Blaauw, M., Christen, J.A., Lopez, M.A.A., Vazquez, J.E., Gonzalez, V.O.M., Belding, T., Theiler, J., Gough, B., Karney, C., 2023. *rbacon*: age-depth modelling using Bayesian statistics. R package version 3.1.1. http://cran.r-project.org/package=rbacon.

Bondar, E.I., Feranchuk, S.I., Miroshnikova, K.A., Sharov, V.V., Kuzmin, D.A., Oreshkova, N.V., Krutovsky, K.V., 2022. Annotation of Siberian larch (*Larix sibirica* Ledeb.) nuclear genome - one of the most cold-resistant tree species in the only deciduous genus in Pinaceae. Plants 11, 2062. https://doi.org/10.3390/plants11152062.

Bova, S., Rosenthal, Y., Liu, Z., Godad, S.P., Yan, M., 2021. Seasonal origin of the thermal maxima at the Holocene and the last interglacial. Nature 589, 548–553. https://doi.org/10.1038/s41586-020-03155-x.

Boyer, F., Mercier, C., Bonin, A., Le Bras, Y., Taberlet, P., Coissac, E., 2016. OBITOOLS: a UNIX-inspired software package for DNA metabarcoding. Mol. Ecol. Resour 16, 176–182. https://doi.org/10.1111/1755-0998.12428.

Briner, J.P., Kaufman, D.S., 2008. Late Pleistocene mountain glaciation in Alaska: key chronologies. J. Quat. Sci. 23, 659–670. https://doi.org/10.1002/jqs.1196.

Brown, J., Ferrians, O., Heginbottom, J.A., Melnikov, E., 2002. Circum-Arctic Map of Permafrost and Ground-Ice Conditions. National Snow and Ice Data Center. https://doi.org/10.7265/skbg-kf16, version 2.

Brubaker, L.B., Anderson, P.M., Edwards, M.E., Lozhkin, A.V., 2005. Beringia as a glacial refugium for boreal trees and shrubs: new perspectives from mapped pollen data. J. Biogeogr. 32, 833–848. https://doi.org/10.1111/j.1365-2699.2004.01203.x.

Capo, E., Giguet-Covex, C., Rouillard, A., Nota, K., Heintzman, P.D., Vuillemin, A., Ariztegui, D., Arnaud, F., Belle, S., Bertilsson, S., Bigler, C., Bindler, R., Brown, A.G., Clarke, C.L., Crump, S.E., Debroas, D., Englund, G., Ficetola, G.F., Garner, R.E., Gauthier, J., Gregory-Eaves, I., Heinecke, L., Herzschuh, U., Ibrahim, A., Kisand, V., Kjær, K.H., Lammers, Y., Littlefair, J., Messager, E., Monchamp, M., Olajos, F., Orsi, W., Pedersen, M.W., Rijal, D.P., Rydberg, J., Spanbauer, T., Stoof-Leichsenring, K.R., Taberlet, P., Talas, L., Thomas, C., Walsh, D.A., Wang, Y., Willerslev, E., van Woerkom, A., Zimmermann, H.H., Coolen, M.J.L., Epp, L.S., Domaizon, I., Alsos, I.G., Parducci, L., 2021. Lake sedimentary DNA research on past terrestrial and aquatic biodiversity: overview and recommendations. Quaternary 4, 6. https://doi.org/10.3390/quat4010006.

Chang, C.Y., Bräutigam, K., Hüner, N.P.A., Ensminger, I., 2021. Champions of winter survival: cold acclimation and molecular regulation of cold hardiness in evergreen conifers. New Phytol. 229, 675–691. https://doi.org/10.1111/nph.16904.

Clark, P.U., Dyke, A.S., Shakun, J.D., Carlson, A.E., Clark, J., Wohlfarth, B., Mitrovica, J. X., Hostetler, S.W., McCabe, A.M., 2009. The last glacial maximum. Science 325, 710–714. https://doi.org/10.1126/science.1172873.

Clarke, C.L., Edwards, M.E., Gielly, L., Ehrich, D., Hughes, P.D.M., Morozova, L.M., Haflidason, H., Mangerud, J., Svendsen, J.I., Alsos, I.G., 2019. Persistence of arctic-alpine flora during 24,000 years of environmental change in the Polar Urals. Sci. Rep. 9, 19613 https://doi.org/10.1038/s41598-019-55989-9.

Cooper, E.J., 2014. Warmer shorter winters disrupt Arctic terrestrial ecosystems. Annu. Rev. Ecol. Evol. Syst. 45, 271–295. https://doi.org/10.1146/annurev-ecolsys-120213-091620.

Courtin, J., Andreev, A.A., Raschke, E., Bala, S., Biskaborn, B.K., Liu, S., Zimmermann, H. H., Diekmann, B., Stoof-Leichsenring, K.R., Pestryakova, L.A., Herzschuh, U., 2021. Vegetation changes in southeastern Siberia during the late pleistocene and the Holocene. Front. Ecol. Evol. 9, 625096 https://doi.org/10.3389/fevo.2021.625096.

Courtin, J., Stoof-Leichsenring, K.R., Lisovski, S., Alsos, I.G., Biskaborn, B.K., Diekmann, B., Melles, M., Wagner, B., Pestryakova, L.A., Russell, J., Huang, Y., Herzschuh, U., 2024. Potential plant extinctions with the loss of the Pleistocene mammoth-steppe. Nat. Commun. in revision.

Croudace, I.W., Rothwell, R.G., 2015. Micro-XRF Studies of Sediment Cores: Applications of a Non-destructive Tool for the Environmental Sciences. Springer, Dordrecht. https://doi.org/10.1007/978-94-017-9849-5.

Dalén, L., Heintzman, P.D., Kapp, J.D., Shapiro, B., 2023. Deep-time paleogenomics and the limits of DNA survival. Science 382, 48–53. https://doi.org/10.1126/science.adh7943.

Diepenbroek, M., Glöckner, F.O., Grobe, P., Güntsch, A., Huber, R., König-Ries, B., Kostadinov, I., Nieschulze, J., Seeger, B., Tolksdorf, R., Triebel, D., 2014. Towards an integrated biodiversity and ecological research data management and archiving platform: the German Federation for the Curation of Biological Data (GFBio). In: Plödereder, E., Grunske, L., Schneider, E., Ull, D. (Eds.), Informatik 2014 - Big Data Komplexität Meistern. GI-Edition: Lecture Notes in Informatics (LNI) - Proceedings, pp. 1711–1724. Köllen Verlag, Bonn. https://dl.gi.de/items/618c1a92-fff2-423e-8c60-a0d6a65fe04f.

Dobrowski, S.Z., 2011. A climatic basis for microrefugia: the influence of terrain on climate. Global Change Biol. 17, 1022–1035. https://doi.org/10.1111/j.1365-2486.2010.02263.x.

Drew, J.W., Bret-Harte, M.S., Buchwal, A., Heslop, C., 2023. Age matters: older *Alnus viridis* ssp. *fruticosa* are more sensitive to summer temperatures in the Alaskan Arctic. Funct. Ecol. 37, 1463–1475. https://doi.org/10.1111/1365-2435.14307.

Dypvik, H., Harris, N.B., 2001. Geochemical facies analysis of fine-grained siliciclastics using Th/U, Zr/Rb and (Zr+Rb)/Sr ratios. Chem. Geol. 181, 131–146. https://doi.org/10.1016/S0009-2541(01)00278-9.

Elias, S.A., Brigham-Grette, J., 2013. Glaciations: late pleistocene glacial events in beringia. In: Elias, S.A., Mock, C.J. (Eds.), Encyclopedia of Quaternary Science, second ed. Elsevier, Amsterdam, pp. 191–201. https://doi.org/10.1016/B978-0-444-53643-3.00116-3.

Elmendorf, S.C., Henry, G.H.R., Hollister, R.D., Björk, R.G., Boulanger-Lapointe, N., Cooper, E.J., Cornelissen, J.H.C., Day, T.A., Dorrepaal, E., Elumeeva, T.G., Gill, M., Gould, W.A., Harte, J., Hik, D.S., Hofgaard, A., Johnson, D.R., Johnstone, J.F., Jónsdóttir, I.S., Jorgenson, J.C., Klanderud, K., Klein, J.A., Koh, S., Kudo, G., Lara, M., Lévesque, E., Magnússon, B., May, J.L., Mercado-Díaz, J.A., Michelsen, A., Molau, U., Myers-Smith, I.H., Oberbauer, S.F., Onipchenko, V.G., Rixen, C., Schmidt, N.M., Shaver, G.R., Spasojevic, M.J., þórhallsdóttir, þ.E., Tolvanen, A., Troxler, T., Tweedie, C.E., Villareal, S., Wahren, C., Walker, X., Webber, P.J., Welker, J.M., Wipf, S., 2012. Plot-scale evidence of tundra vegetation change and links to recent summer warming. Nat. Clim. Change 2, 453–457. https://doi.org/10.1038/nclimate1465.

Epp, L.S., Zimmermann, H.H., Stoof-Leichsenring, K.R., 2019. Sampling and extraction of ancient DNA from sediments. In: Shapiro, B., Barlow, A., Heintzman, P.D., Hofreiter, M., Paijmans, J.L.A., Soares, A.E.R. (Eds.), Ancient DNA: Methods and Protocols, second ed. Springer, New York. https://doi.org/10.1007/978-1-4939-9176-1_5.

Ernakovich, J.G., Hopping, K.A., Berdanier, A.B., Simpson, R.T., Kachergis, E.J., Steltzer, H., Wallenstein, M.D., 2014. Predicted responses of arctic and alpine ecosystems to altered seasonality under climate change. Global Change Biol. 20, 3256–3269. https://doi.org/10.1111/gcb.12568.

Feurdean, A., Bhagwat, S.A., Willis, K.J., Birks, H.J.B., Lischke, H., Hickler, T., 2013. Tree migration-rates: narrowing the gap between inferred post-glacial rates and projected rates. PLoS One 8, e71797. https://doi.org/10.1371/journal.pone.0071797.

Folk, R.A., Siniscalchi, C.M., Soltis, D.E., 2020. Angiosperms at the edge: extremity, diversity, and phylogeny. Plant Cell Environ. 43, 2871–2893. https://doi.org/10.1111/pce.13887.

Garcés-Pastor, S., Nota, K., Rijal, D.P., Liu, S., Jia, W., Leunda, M., Schwörer, C., Crump, S.E., Parducci, L., Alsos, I.G., 2023. Terrestrial plant DNA from lake sediments. In: Capo, E., Barouillet, C., Smol, J.P. (Eds.), Tracking Environmental Change Using Lake Sediments Volume 6. Sedimentary DNA. Springer, Cham, pp. 275–298. https://doi.org/10.1007/978-3-031-43799-1_10.

Giguet-Covex, C., Ficetola, G.F., Walsh, K., Poulenard, J., Bajard, M., Fouinat, L., Sabatier, P., Gielly, L., Messager, E., Develle, A.L., David, F., Taberlet, P., Brisset, E., Guiter, F., Sinet, R., Arnaud, F., 2019. New insights on lake sediment DNA from the catchment: importance of taphonomic and analytical issues on the record quality. Sci. Rep. 9, 14676 https://doi.org/10.1038/s41598-019-50339-1.

Gowan, E.J., Zhang, X., Khosravi, S., Rovere, A., Stocchi, P., Hughes, A.L.C., Gyllencreutz, R., Mangerud, J., Svendsen, J., Lohmann, G., 2021. A new global ice sheet reconstruction for the past 80 000 years. Nat. Commun. 12, 1199. https://doi.org/10.1038/s41467-021-21469-w.

Griffith, M., Yaish, M.W.F., 2004. Antifreeze proteins in overwintering plants: a tale of two activities. Trends Plant Sci. 9, 399–405. https://doi.org/10.1016/j.tplants.2004.06.007.

Gupta, R., Deswal, R., 2014. Antifreeze proteins enable plants to survive in freezing conditions. J. Biosci. 39, 931–944. https://doi.org/10.1007/s12038-014-9468-2.

Herzschuh, U., 2020. Legacy of the Last Glacial on the present-day distribution of deciduous versus evergreen boreal forests. Global Ecol. Biogeogr. 29, 198–206. https://doi.org/10.1111/geb.13018.

Herzschuh, U., Birks, H.J.B., Laepple, T., Andreev, A., Melles, M., Brigham-Grette, J., 2016. Glacial legacies on interglacial vegetation at the Pliocene-Pleistocene transition in NE Asia. Nat. Commun. 7, 11967 https://doi.org/10.1038/ncomms11967.

Herzschuh, U., Li, C., Böhmer, T., Postl, A.K., Heim, B., Andreev, A.A., Cao, X., Wieczorek, M., Ni, J., 2022. LegacyPollen 1.0: a taxonomically harmonized global late Quaternary pollen dataset of 2831 records with standardized chronologies. Earth Syst. Sci. Data 14, 3213–3227. https://doi.org/10.5194/essd-14-3213-2022.

Huang, S., Stoof-Leichsenring, K.R., Liu, S., Courtin, J., Andreev, A.A., Pestryakova, L.A., Herzschuh, U., 2021. Plant sedimentary ancient DNA from far east Russia covering the last 28,000 years reveals different assembly rules in cold and warm climates. Front. Ecol. Evol. 9, 763747 https://doi.org/10.3389/fevo.2021.763747.

Intergovernmental Panel on Climate Change (IPCC), 2023. Climate Change 2022 - Impacts, Adaptation and Vulnerability: Working Group II Contribution to the Sixth Assessment Report of the Intergovernmental Panel on Climate Change. Cambridge University Press, Cambridge. https://doi.org/10.1017/9781009325844.

Isaia, I., 2016. Regional particularities of the Metonic meteorological cycle on Earth. Pres. Environ. Dev. Sustain. 10, 119–132. https://doi.org/10.1515/pesd-2016-0030.

Jia, W., Anslan, S., Chen, F., Cao, X., Dong, H., Dulias, K., Gu, Z., Heinecke, L., Jiang, H., Kruse, S., Kang, W., Li, K., Liu, S., Liu, X., Liu, Y., Ni, J., Schwalb, A., Stoof-Leichsenring, K.R., Shen, W., Tian, F., Wang, J., Wang, Y., Wang, Y., Xu, H., Yang, X., Zhang, D., Herzschuh, U., 2022. Sedimentary ancient DNA reveals past ecosystem and biodiversity changes on the Tibetan Plateau: overview and prospects. Quat. Sci. Rev. 293, 107703 https://doi.org/10.1016/j.quascirev.2022.107703.

Jonczak, J., Jankiewicz, U., Kondras, M., Kruczkowska, B., Oktaba, L., Oktaba, J., Olejniczak, I., Pawłowicz, E., Polláková, N., Raab, T., Regulska, E., Słowińska, S., Sut-Lohmann, M., 2020. The influence of birch trees (*Betula* spp.) on soil environment - a review. For. Ecol. Manage. 477, 118486 https://doi.org/10.1016/j.foreco.2020.118486.

Kanz, C., Aldebert, P., Althorpe, N., Baker, W., Baldwin, A., Bates, K., Browne, P., van den Broek, A., Castro, M., Cochrane, G., Duggan, K., Eberhardt, R., Faruque, N., Gamble, J., Diez, F.G., Harte, N., Kulikova, T., Lin, Q., Lombard, V., Lopez, R., Mancuso, R., McHale, M., Nardone, F., Silventoinen, V., Sobhany, S., Stoehr, P., Tuli, M.A., Tzouvara, K., Vaughan, R., Wu, D., Zhu, W., Apweiler, R., 2005. The EMBL nucleotide sequence database. Nucleic Acids Res. 33, D29–D33. https://doi.org/10.1093/nar/gki098.

Kaufman, D.S., Broadman, E., 2023. Revisiting the Holocene global temperature conundrum. Nature 614, 425–435. https://doi.org/10.1038/s41586-022-05536-w.

Kienast, F., Schirrmeister, L., Siegert, C., Tarasov, P., 2005. Palaeobotanical evidence for warm summers in the East Siberian Arctic during the last cold stage. Quat. Res. 63, 283–300. https://doi.org/10.1016/j.yqres.2005.01.003.

Kreyling, J., Grant, K., Hammerl, V., Arfin-Khan, M.A.S., Malyshev, A.V., Peñuelas, J., Pritsch, K., Sardans, J., Schloter, M., Schuerings, J., Jentsch, A., Beierkuhnlein, C., 2019. Winter warming is ecologically more relevant than summer warming in a cool-temperate grassland. Sci. Rep. 9, 14632 https://doi.org/10.1038/s41598-019-51221-w.

Kruse, S., Kolmogorov, A.I., Pestryakova, L.A., Herzschuh, U., 2020. Long-lived larch clones may conserve adaptations that could restrict treeline migration in northern Siberia. Ecol. Evol. 10, 10017–10030. https://doi.org/10.1002/ece3.6660.

Kwiecien, O., Braun, T., Brunello, C.F., Faulkner, P., Hausmann, N., Helle, G., Hoggarth, J.A., Ionita, M., Jazwa, C.S., Kelmelis, S., Marwan, N., Nava-Fernandez, C., Nehme, C., Opel, T., Oster, J.L., Perşoiu, A., Petrie, C., Prufer, K., Saarni, S.M., Wolf, A., Breitenbach, S.F.M., 2022. What we talk about when we talk about seasonality - a transdisciplinary review. Earth Sci. Rev. 225, 103843 https://doi.org/10.1016/j.earscirev.2021.103843.

Laepple, T., Werner, M., Lohmann, G., 2011. Synchronicity of Antarctic temperatures and local solar insolation on orbital timescales. Nature 471, 91–94. https://doi.org/10.1038/nature09825.

Lapointe, E.L., Talbot, J., Fortier, D., Fréchette, B., Strauss, J., Kanevskiy, M., Shur, Y., 2017. Middle to late wisconsinan climate and ecological changes in northern Alaska: evidences from the itkillik river yedoma. Palaeogeogr. Palaeoclimatol. Palaeoecol. 485, 906–916. https://doi.org/10.1016/j.palaeo.2017.08.006.

Larson, R.A., Brooks, G.R., Devine, B., Schwing, P.T., Holmes, C.W., Jilbert, T., Reichart, G., 2015. Elemental signature of terrigenous sediment runoff as recorded in coastal salt ponds: US Virgin Islands. Appl. Geochem. 63, 573–585. https://doi.org/10.1016/j.apgeochem.2015.01.008.

Laskar, J., Robutel, P., Joutel, F., Gastineau, M., Correia, A.C.M., Levrard, B., 2004. A long-term numerical solution for the insolation quantities of the Earth. Astron. Astrophys. 428, 261–285. https://doi.org/10.1051/0004-6361:20041335.

Leng, M.J., Marshall, J.D., 2004. Palaeoclimate interpretation of stable isotope data from lake sediment archives. Quat. Sci. Rev. 23, 811–831. https://doi.org/10.1016/j.quascirev.2003.06.012.

Legendre, P., Birks, H.J.B., 2012. From classical to canonical ordination. In: Birks, H.J.B., Lotter, A.F., Juggins, S., Smol, J.P. (Eds.), Tracking Environmental Change Using Lake Sediments Volume 5: Data Handling and Numerical Techniques. Springer, Dordrecht, pp. 201–248. https://doi.org/10.1007/978-94-007-2745-8_8.

Liu, S., Kruse, S., Scherler, D., Ree, R.H., Zimmermann, H.H., Stoof-Leichsenring, K.R., Epp, L.S., Mischke, S., Herzschuh, U., 2021. Sedimentary ancient DNA reveals a threat of warming-induced alpine habitat loss to Tibetan Plateau plant diversity. Nat. Commun. 12, 2995. https://doi.org/10.1038/s41467-021-22986-4.

Liu, X., Dong, H., Yang, X., Herzschuh, U., Zhang, E., Stuut, J.W., Wang, Y., 2009. Late Holocene forcing of the Asian winter and summer monsoon as evidenced by proxy records from the northern Qinghai-Tibetan Plateau. Earth Planet Sci. Lett. 280, 276–284. https://doi.org/10.1016/j.epsl.2009.01.041.

Liu, X., Herzschuh, U., Wang, Y., Kuhn, G., Yu, Z., 2014. Glacier fluctuations of Muztagh Ata and temperature changes during the late Holocene in westernmost Tibetan Plateau, based on glaciolacustrine sediment records. Geophys. Res. Lett. 41, 6265–6273. https://doi.org/10.1002/2014GL060444.

Lozhkin, A., Anderson, P., Minyuk, P., Korzun, J., Brown, T., Pakhomov, A., Tsygankova, V., Burnatny, S., Naumov, A., 2018. Implications for conifer glacial refugia and postglacial climatic variation in western Beringia from lake sediments of the Upper Indigirka basin. Boreas 47, 938–953. https://doi.org/10.1111/bor.12316.

Margold, M., Jansen, J.D., Gurinov, A.L., Codilean, A.T., Fink, D., Preusser, F., Reznichenko, N.V., Mifsud, C., 2016. Extensive glaciation in transbaikalia, Siberia, at the last glacial maximum. Quat. Sci. Rev. 132, 161–174. https://doi.org/10.1016/j.quascirev.2015.11.018.

Meyer, H., Opel, T., Laepple, T., Dereviagin, A.Y., Hoffmann, K., Werner, M., 2015. Long-term winter warming trend in the Siberian Arctic during the mid- to late Holocene. Nat. Geosci. 8, 122–125. https://doi.org/10.1038/ngeo2349.

Meyers, P.A., 2001. Sediment organic matter. In: Last, W.M., Smol, J.P. (Eds.), Tracking Environmental Change Using Lake Sediments Volume 2: Physical and Geochemical Methods. Springer, Dordrecht, pp. 239–269. https://doi.org/10.1007/0-306-47670-3.

Miesner, T., Herzschuh, U., Pestryakova, L.A., Wieczorek, M., Zakharov, E.S., Kolmogorov, A.I., Davydova, P.V., Kruse, S., 2022. Forest structure and individual tree inventories of northeastern Siberia along climatic gradients. Earth Syst. Sci. Data 14, 5695–5716. https://doi.org/10.5194/essd-14-5695-2022.

Miller, G.H., Alley, R.B., Brigham-Grette, J., Fitzpatrick, J.J., Polyak, L., Serreze, M.C., White, J.W.C., 2010. Arctic amplification: can the past constrain the future? Quat. Sci. Rev. 29, 1779–1790. https://doi.org/10.1016/j.quascirev.2010.02.008.

Ministry for Natural Resources and Ecology of the Russian Federation, 2011. Geological Map of Russia and adjoining water areas. Scale 1 (2), 500,000. https://www.vsegei.ru/ru/info/gk-2500/index.php.

Ministry for Natural Resources and Ecology of the Russian Federation, 2014. Map of the quaternary formations of the Russian federation, scale 1:2,500,000. https://vsegei.ru/ru/info/quaternary-2500.

Mollenhauer, G., Grotheer, H., Gentz, T., Bonk, E., Hefter, J., 2021. Standard operation procedures and performance of the MICADAS radiocarbon laboratory at Alfred Wegener Institute (AWI), Germany. Nucl. Instrum. Methods Phys. Res. B. 496, 45–51. https://doi.org/10.1016/j.nimb.2021.03.016.

Naeher, S., Gilli, A., North, R.P., Hamann, Y., Schubert, C.J., 2013. Tracing bottom water oxygenation with sedimentary Mn/Fe ratios in Lake Zurich, Switzerland. Chem. Geol. 352, 125–133. https://doi.org/10.1016/j.chemgeo.2013.06.006.

Niemeyer, B., Epp, L.S., Stoof-Leichsenring, K.R., Pestryakova, L.A., Herzschuh, U., 2017. A comparison of sedimentary DNA and pollen from lake sediments in recording vegetation composition at the Siberian treeline. Mol. Ecol. Resour 17, e46–e62. https://doi.org/10.1111/1755-0998.12689.

Niemeyer, B., Klemm, J., Pestryakova, L.A., Herzschuh, U., 2015. Relative pollen productivity estimates for common taxa of the northern Siberian Arctic. Rev. Palaeobot. Palynol. 221, 71–82. https://doi.org/10.1016/j.revpalbo.2015.06.008.

Niittynen, P., Heikkinen, R.K., Aalto, J., Guisan, A., Kemppinen, J., Luoto, M., 2020. Fine-scale tundra vegetation patterns are strongly related to winter thermal conditions. Nat. Clim. Change 10, 1143–1148. https://doi.org/10.1038/s41558-020-00916-4.

Oberhuber, W., Wieser, G., Bernich, F., Gruber, A., 2022. Radial stem growth of the clonal shrub *Alnus alnobetula* at treeline is constrained by summer temperature and winter desiccation and differs in carbon allocation strategy compared to co-occurring *Pinus cembra*. Forests 13, 440. https://doi.org/10.3390/f13030440.

Oksanen, J., Simpson, G.L., Blanchet, F.G., Kindt, R., Legendre, P., Minchin, P.R., O'Hara, R.B., Solymos, P., Stevens, M.H.H., Szoecs, E., Wagner, H., Barbour, M., Bedward, M., Bolker, B., Borcard, D., Carvalho, G., Chirico, M., De Caceres, M., Durand, S., Evangelista, H.B.A., FitzJohn, R., Friendly, M., Furneaux, B., Hannigan, G., Hill, M.O., Lahti, L., McGlinn, D., Ouellette, M., Cunha, E.R., Smith, T., Stier, A., Ter Braak, C.J.F., Weedon, J., 2022. *vegan*: community ecology package. R package version 2, 6-4. http://cran.r-project.org/package=vegan.

Pedersen, M.W., Ruter, A., Schweger, C., Friebe, H., Staff, R.A., Kjeldsen, K.K., Mendoza, M.L.Z., Beaudoin, A.B., Zutter, C., Larsen, N.K., Potter, B.A., Nielsen, R., Rainville, R.A., Orlando, L., Meltzer, D.J., Kjær, K.H., Willerslev, E., 2016. Postglacial viability and colonization in North America's ice-free corridor. Nature 537, 45–49. https://doi.org/10.1038/nature19085.

Piao, S., Liu, Q., Chen, A., Janssens, I.A., Fu, Y., Dai, J., Liu, L., Lian, X., Shen, M., Zhu, X., 2019. Plant phenology and global climate change: current progresses and challenges. Global Change Biol. 25, 1922–1940. https://doi.org/10.1111/gcb.14619.

Ponomarev, E.I., Kharuk, V.I., Ranson, K.J., 2016. Wildfires dynamics in Siberian larch forests. Forests 7, 125. https://doi.org/10.3390/f7060125.

R Core Team, 2023. R: A Language and Environment for Statistical Computing. R Foundation for Statistical Computing, Vienna, Austria. http://www.r-project.org.

Rapacz, M., Ergon, Å., Höglind, M., Jørgensen, M., Jurczyk, B., Østrem, L., Rognli, O.A., Tronsmo, A.M., 2014. Overwintering of herbaceous plants in a changing climate. Still more questions than answers. Plant Sci. 225, 34–44. https://doi.org/10.1016/j.plantsci.2014.05.009.

Reimer, P.J., Austin, W.E.N., Bard, E., Bayliss, A., Blackwell, P.G., Ramsey, C.B., Butzin, M., Cheng, H., Edwards, R.L., Friedrich, M., Grootes, P.M., Guilderson, T.P., Hajdas, I., Heaton, T.J., Hogg, A.G., Hughen, K.A., Kromer, B., Manning, S.W., Muscheler, R., Palmer, J.G., Pearson, C., van der Plicht, J., Reimer, R.W., Richards, D.A., Scott, E.M., Southon, J.R., Turney, C.S.M., Wacker, L., Adolphi, F., Büntgen, U., Capano, M., Fahrni, S.M., Fogtmann-Schulz, A., Friedrich, R., Köhler, P., Kudsk, S., Miyake, F., Olsen, J., Reinig, F., Sakamoto, M., Sookdeo, A., Talamo, S., 2020. The IntCal20 Northern Hemisphere radiocarbon age calibration curve (0–55 cal kBP). Radiocarbon 62, 725–757. https://doi.org/10.1017/RDC.2020.41.

Revelle, W., 2023. *psych*: procedures for psychological, psychometric, and personality research. R package version 2 (3.9). http://cran.r-project.org/package=psych.

Revéret, A., Rijal, D.P., Heintzman, P.D., Brown, A.G., Stoof-Leichsenring, K.R., Alsos, I. G., 2023. Environmental DNA of aquatic macrophytes: the potential for reconstructing past and present vegetation and environments. Freshw. Biol. 68, 1929–1950. https://doi.org/10.1111/fwb.14158.

RStudio Team, 2020. RStudio: integrated development for R. http://www.rstudio.com.

Sanders-DeMott, R., Templer, P.H., 2017. What about winter? Integrating the missing season into climate change experiments in seasonally snow covered ecosystems. Methods Ecol. Evol. 8, 1183–1191. https://doi.org/10.1111/2041-210X.12780.

Schönswetter, P., Stehlik, I., Holderegger, R., Tribsch, A., 2005. Molecular evidence for glacial refugia of mountain plants in the European Alps. Mol. Ecol. 14, 3547–3555. https://doi.org/10.1111/j.1365-294X.2005.02683.x.

Schuchardt, M.A., Berauer, B.J., von Heßberg, A., Wilfahrt, P., Jentsch, A., 2021. Drought effects on montane grasslands nullify benefits of advanced flowering phenology due to warming. Ecosphere 12, e03661. https://doi.org/10.1002/ecs2.3661.

Schulte, L., Li, C., Lisovski, S., Herzschuh, U., 2022a. Forest-permafrost feedbacks and glacial refugia help explain the unequal distribution of larch across continents. J. Biogeogr. 49, 1825–1838. https://doi.org/10.1111/jbi.14456.

Schulte, L., Meucci, S., Stoof-Leichsenring, K.R., Heitkam, T., Schmidt, N., von Hippel, B., Andreev, A.A., Diekmann, B., Biskaborn, B.K., Wagner, B., Melles, M., Pestryakova, L.A., Alsos, I.G., Clarke, C., Krutovsky, K.V., Herzschuh, U., 2022b. *Larix* species range dynamics in Siberia since the Last Glacial captured from sedimentary ancient DNA. Commun. Biol. 5, 570. https://doi.org/10.1038/s42003-022-03455-0.

Schulze, E., Wirth, C., Mollicone, D., von Lüpke, N., Ziegler, W., Achard, F., Mund, M., Prokushkin, A., Scherbina, S., 2012. Factors promoting larch dominance in central Siberia: fire versus growth performance and implications for carbon dynamics at the boundary of evergreen and deciduous conifers. Biogeosciences 9, 1405–1421. https://doi.org/10.5194/bg-9-1405-2012.

Sjögren, P., Edwards, M.E., Gielly, L., Langdon, C.T., Croudace, I.W., Merkel, M.K.F., Fonville, T., Alsos, I.G., 2017. Lake sedimentary DNA accurately records 20$^{th}$ Century introductions of exotic conifers in Scotland. New Phytol. 213, 929–941. https://doi.org/10.1111/nph.14199.

Sjögren, P., van der Knaap, W.O., Huusko, A., van Leeuwen, J.F.N., 2008. Pollen productivity, dispersal, and correction factors for major tree taxa in the Swiss Alps based on pollen-trap results. Rev. Palaeobot. Palynol. 152, 200–210. https://doi.org/10.1016/j.revpalbo.2008.05.003.

Soininen, E.M., Gauthier, G., Bilodeau, F., Berteaux, D., Gielly, L., Taberlet, P., Gussarova, G., Bellemain, E., Hassel, K., Stenøien, H.K., Epp, L.S., Schrøder-Nielsen, A., Brochmann, C., Yoccoz, N.G., 2015. Highly overlapping winter diet in two sympatric lemming species revealed by DNA metabarcoding. PLoS One 10, e0115335. https://doi.org/10.1371/journal.pone.0115335.

Sønstebø, J.H., Gielly, L., Brysting, A.K., Elven, R., Edwards, M., Haile, J., Willerslev, E., Coissac, E., Rioux, D., Sannier, J., Taberlet, P., Brochmann, C., 2010. Using next-generation sequencing for molecular reconstruction of past Arctic vegetation and climate. Mol. Ecol. Resour 10, 1009–1018. https://doi.org/10.1111/j.1755-0998.2010.02855.x.

Spratt, R.M., Lisiecki, L.E., 2016. A Late Pleistocene sea level stack. Clim. Past 12, 1079–1092. https://doi.org/10.5194/cp-12-1079-2016.

Starr, G.R.E., Oberbauer, S.F., Pop, E.R.I.C.W., 2001. Effects of lengthened growing season and soil warming on the phenology and physiology of *Polygonum bistorta*. Global Change Biol. 6, 357–369. https://doi.org/10.1046/j.1365-2486.2000.00316.x.

Stewart, J.R., Lister, A.M., Barnes, I., Dalén, L., 2010. Refugia revisited: individualistic responses of species in space and time. Proc. R. Soc. A B. 277, 661–671. https://doi.org/10.1098/rspb.2009.1272.

Stoof-Leichsenring, K.R., Huang, S., Liu, S., Jia, W., Li, K., Liu, X., Herzschuh, U., 2022. Sedimentary DNA identifies modern and past macrophyte diversity and its environmental drivers in high-latitude and high-elevation lakes in Siberia and China. Limnol. Oceanogr. 67, 1126–1141. https://doi.org/10.1002/lno.12061.

Stoof-Leichsenring, K.R., Liu, S., Jia, W., Li, K., Pestryakova, L.A., Mischke, S., Cao, X., Liu, X., Ni, J., Neuhaus, S., Herzschuh, U., 2020. Plant diversity in sedimentary DNA obtained from high-latitude (Siberia) and high-elevation lakes (China). Biodivers. Data J. 8, e57089 https://doi.org/10.3897/BDJ.8.e57089.

Taberlet, P., Coissac, E., Pompanon, F., Gielly, L., Miquel, C., Valentini, A., Vermat, T., Corthier, G., Brochmann, C., Willerslev, E., 2007. Power and limitations of the chloroplast *trn*L (UAA) intron for plant DNA barcoding. Nucleic Acids Res. 35, e14. https://doi.org/10.1093/nar/gkl938.

van den Boogaart, K.G., Tolosana-Delgado, R., Bren, M., 2023. *compositions*: compositional data analysis. R package version 2.0–6. http://cran.r-project.org/package=compositions.

von Hippel, B., Stoof-Leichsenring, K.R., Schulte, L., Seeber, P., Epp, L.S., Biskaborn, B. K., Diekmann, B., Melles, M., Pestryakova, L., Herzschuh, U., 2022. Long-term fungus-plant covariation from multi-site sedimentary ancient DNA metabarcoding. Quat. Sci. Rev. 295, 107758 https://doi.org/10.1016/j.quascirev.2022.107758.

Vyse, S.A., Herzschuh, U., Andreev, A.A., Pestryakova, L.A., Diekmann, B., Armitage, S. J., Biskaborn, B.K., 2020. Geochemical and sedimentological responses of arctic glacial Lake Ilirney, chukotka (far east Russia) to palaeoenvironmental change since ~51.8 ka BP. Quat. Sci. Rev. 247, 106607 https://doi.org/10.1016/j.quascirev.2020.106607.

Weltje, G.J., Tjallingii, R., 2008. Calibration of XRF core scanners for quantitative geochemical logging of sediment cores: theory and application. Earth Planet Sci. Lett. 274, 423–438. https://doi.org/10.1016/j.epsl.2008.07.054.

White, E.R., Hastings, A., 2020. Seasonality in ecology: progress and prospects in theory. Ecol. Complex. 44, 100867 https://doi.org/10.1016/j.ecocom.2020.100867.

Willerslev, E., Davison, J., Moora, M., Zobel, M., Coissac, E., Edwards, M.E., Lorenzen, E. D., Vestergård, M., Gussarova, G., Haile, J., Craine, J., Gielly, L., Boessenkool, S., Epp, L.S., Pearman, P.B., Cheddadi, R., Murray, D., Bråthen, K.A., Yoccoz, N., Binney, H., Cruaud, C., Wincker, P., Goslar, T., Alsos, I.G., Bellemain, E., Brysting, A. K., Elven, R., Sønstebø, J.H., Murton, J., Sher, A., Rasmussen, M., Rønn, R., Mourier, T., Cooper, A., Austin, J., Möller, P., Froese, D., Zazula, G., Pompanon, F., Rioux, D., Niderkorn, V., Tikhonov, A., Savvinov, G., Roberts, R.G., MacPhee, R.D.E., Gilbert, M.T.P., Kjær, K.H., Orlando, L., Brochmann, C., Taberlet, P., 2014. Fifty thousand years of Arctic vegetation and megafaunal diet. Nature 506, 47–51. https://doi.org/10.1038/nature12921.

Williams, C.M., Henry, H.A.L., Sinclair, B.J., 2015. Cold truths: how winter drives responses of terrestrial organisms to climate change. Biol. Rev. 90, 214–235. https://doi.org/10.1111/brv.12105.

Wisniewski, M., Willick, I.R., Duman, J.G., Livingston III, D., Newton, S.S., 2020. Plant antifreeze proteins. In: Ramløv, H., Friis, D.S. (Eds.), Antifreeze Proteins Volume 1: Environment, Systematics and Evolution. Springer, Cham, pp. 189–226. https://doi.org/10.1007/978-3-030-41929-5_7.

Wunderlich, J., Müller, S., 2003. High-resolution sub-bottom profiling using parametric acoustics. Int. Ocean Syst. 7, 6–11. https://innomar.com/upload/publications/2003_oceansystems.pdf.

Xia, J., Chen, J., Piao, S., Ciais, P., Luo, Y., Wan, S., 2014. Terrestrial carbon cycle affected by non-uniform climate warming. Nat. Geosci. 7, 173–180. https://doi.org/10.1038/ngeo2093.

Zhang, Y., Piao, S., Sun, Y., Rogers, B.M., Li, X., Lian, X., Liu, Z., Chen, A., Peñuelas, J., 2022. Future reversal of warming-enhanced vegetation productivity in the Northern Hemisphere. Nat. Clim. Change 12, 581–586. https://doi.org/10.1038/s41558-022-01374-w.

Zimmermann, H.H., Raschke, E., Epp, L.S., Stoof-Leichsenring, K.R., Schwamborn, G., Schirrmeister, L., Overduin, P.P., Herzschuh, U., 2017. Sedimentary ancient DNA and pollen reveal the composition of plant organic matter in Late Quaternary permafrost sediments of the Buor Khaya Peninsula (north-eastern Siberia). Biogeosciences 14, 575–596. https://doi.org/10.5194/bg-14-575-2017.

Zolitschka, B., Francus, P., Ojala, A.E.K., Schimmelmann, A., 2015. Varves in lake sediments - a review. Quat. Sci. Rev. 117, 1–41. https://doi.org/10.1016/j.quascirev.2015.03.019.